

Delta-DOR: The One-Nanoradian Navigation Measurement System of the Deep Space Network — History, Architecture, and Componentry

David W. Curkendall* and James S. Border†

ABSTRACT. — Doppler and range data alone supported navigation for the earliest missions into deep space. Though extremely precise in line-of-sight coordinates, the navigation system built on these data had a weakness for determining the spacecraft declination component. To address this, the Deep Space Network (DSN) developed the capability for very long baseline interferometry measurements beginning in the late 1970s. Both the implementation of the interferometric system and the importance of such measurements to flight projects have evolved significantly over the past three decades. Innovations introduced through research and development programs have led to continuous improvements in performance. Today's system provides data approaching one-nanoradian accuracy with reliability of 98 percent. This article provides an overview of the development and use of interferometric tracking techniques in the DSN starting with the Viking era and continuing with a description of the current system and its planned use to support interplanetary cruise navigation of the Mars Science Laboratory spacecraft.

I. Introduction

From the earliest of times, to chart the heavens meant to take angular measurements of celestial objects. The most important of these were to measure the positions and movements of the planets and of our own Moon. Through Kepler's laws and ultimately with the machinery of Newtonian mechanics, these measurements were turned into ephemerides that could use the measurements of today and predict those for tomorrow. In this way, accurate maps of the solar system were ultimately constructed, all embedded in a reference frame of stars. Modern angular optical measurements were (and are) accurate to on the order of 0.1" or 0.5 microradian (μrad). What was not well measured by these methods was the *scale* of

* Former manager, Tracking Systems and Applications Section, 1980–1981. He went on to hold other management positions at JPL; he retired from JPL in 2004 but continued to work on several projects through 2010. He passed away in 2011.

† Tracking Systems and Applications Section.

The research described in this publication was carried out by the Jet Propulsion Laboratory, California Institute of Technology, under a contract with the National Aeronautics and Space Administration. © 2013 California Institute of Technology. U.S. Government sponsorship acknowledged.

the solar system, and this was essentially the distance, say, between Earth and the Sun, i.e., the astronomical unit (AU). If we had known the mass of the Sun, Newtonian mechanics could have provided this scale, but that too was unknown; the model solar system lacked this one essential constant.

The literature is replete with attempts to measure the AU [1]; most devolved to knowing or measuring the size of Earth and then posting two observers at disparate locations on it and measuring the parallax when observing the transit of Venus or some other object across the face of the Sun — i.e., when Venus first touches the limb of the Sun from the point of view of one observer, how far distant is it as seen from the other? Clever, but not particularly accurate; the AU continued to be uncertain — Halley claimed about 1 part in 500 but successive experiments continued to give new answers spaced farther apart than that.¹ The situation remained this way until the beginnings of interplanetary spaceflight. Then, just before the Mariner launch window to Venus opened in July 1962, JPL completed preparations for a planetary radar system at Goldstone, California, and Richard Goldstein successfully detected Venus that April, making the first direct radiometric measurement of the scale of the solar system [2].

This measurement, plus its refinement afforded via tracking Mariner II during its Venusian close encounter, reversed the earlier situation — scale became the best-measured quantity rather than the worst. By 1968, the AU was known to an accuracy of 15 microseconds (μs), or 0.03 microparts/part, as quoted by Melbourne [3]. Moreover, since the AU was now measured by light travel time between the planets, the reference unit of determination changed from Earth radii to light-seconds.

But if the radiometric techniques introduced for tracking spacecraft — first, coherent two-way Doppler and later, two-way range — measured velocity and distance to heretofore undreamed of accuracies, they suffered a much poorer ability to take angular measurements. The Fresnel diffraction limit of optical telescopes — $\sim 0.1 \mu\text{rad}$ — was substituted by a 2.3-GHz (S-band) angular precision of on the order of 2 milliradians for even the largest telescopes of the Deep Space Network (DSN). That numerical simulations of orbit determination predicted much higher accuracies and early flight experiments proved them correct were, for a time, a welcome mystery. The mystery was solved first by Jay Light [4], who noticed that there was an interaction between the rotational movement of the tracking stations and the Doppler dependency on the spacecraft's angular position; this was first called *velocity parallax*. Hamilton–Melbourne [5] further developed these observations with their definitive paper taking an *information content* point of view and describing analytically the ability to determine right ascension, declination, and its accuracy dependence on the nominal declination itself. Today, we would probably describe this phenomenon in terms of *aperture synthesis*; i.e., it is the tracking stations' displacement during the observation time that permits an aperture synthesis and, in effect, permits us to substitute the near diameter of Earth for the antenna diameter in computing the Fresnel diffraction limits. The inherent angular precision that becomes possible is then on the order of 10 nanoradians (nrad) at S-band, and much higher at 8.4 GHz (X-band) and 32 GHz (Ka-band).

¹ Transits of Venus are remarkably rare. They usually come in pairs with spacing of eight years, with the pairs themselves repeating fewer than once per century.

The Hamilton–Melbourne analysis was highly successful at informing and guiding the understanding of Doppler tracking accuracy and sensitivities to both errors and to geometry — the ability to determine declination vanishes at and near zero spacecraft declination — for the early portions of planetary exploration. A significant ongoing effort was made to characterize the inherent accuracy of the radiometric data and the influence of its many error sources that kept its performance short of this inherent performance. The contributions of errors in the DSN station locations, Universal Time (UT), polar motion (PM), errors introduced via the media — troposphere, ionosphere — the effect of oscillator instability, even the effect of numerical precision of the orbit-determination software, were all studied and efforts to calibrate and control these errors were mounted. As a result, the accuracy of interplanetary navigation increased steadily throughout the 1960s and 1970s. And the flight projects in turn designed more demanding and rewarding missions to take advantage of these advances.

By the early 1970s, station locations were known to under 2 m, and calibrated S-/X-band Doppler was accurate to 1 mm/s, or more importantly, had integrated errors over a pass of less than 1.5 m. Thus, for all but the lowest of declination geometries, the system could deliver Earth-relative navigation accuracy approaching $0.25 \mu\text{rad}$.

Voyager, to be launched in 1977, proved particularly demanding. It was to be JPL's first precision venture beyond the terrestrial planets and the increased distances meant the still optically determined outer planet ephemerides would contain commensurately larger Earth-relative errors. Worse, the encounter at Saturn was to take place at near-zero declination; Doppler data alone would be ineffective. To meet these challenges, four separate development efforts were defined:

- A worldwide effort to observe the outer planets and their satellites was enlisted, ensuring their ephemerides were reliably determined to that 0.1-arcsecond level.
- The development of nearly simultaneous two-way ranging. This was seen as the proper means to introduce very long baseline interferometry (VLBI) concepts to radiometric spacecraft tracking. The effective differencing of these measurements from stations ~10,000 km distant from one another could achieve direct measurements of spacecraft declination and make up for the Doppler's inability to "see" at zero declination. A goal of 5 m in ranging accuracy was set for the Voyager Saturn encounters.
- Onboard optical navigation. Spacecraft imaging of the planet's satellites fixed in a star background was made operational and was seen as the means to achieve target-relative navigation for the outer planets irrespective of the limits on terrestrial tracking and ephemerides determination [6].
- Analytic theories of satellite motion for both Jupiter's and Saturn's satellites were developed by Lieske [7], enabling near-real-time differential correction to the satellite ephemerides as the optical data were received during approach.

VLBI was developed as the means for routinely providing station locations and calibrations for UT/PM. It was seen also as a means of achieving station clock synchronization but, since the two-way data types were insensitive to this error, this was secondary. The navigation

and VLBI systems were on independent development paths, but the VLBI development was largely in support of the spacecraft navigation requirements.²

The nearly simultaneous range development proved more difficult than expected. Early tests of the differenced range accuracy showed performances closer to 50 m rather than the $\sqrt{2} * 5$ m goal, and it was determined that part of the difficulty lay in the use of square-wave modulation of the ranging code itself. The harmonics of this modulation, particularly as they reached the bandpass limits of the system, proved difficult to calibrate for station instrumentation and spacecraft delay characteristics. A more far-reaching difficulty was the rather narrow bandwidth of the ranging signal itself — approximately 0.5 MHz fundamental. This was fine when the objective was to measure the range to the spacecraft — a few meters made that position component the most accurately measured of the three. What it was not good for was providing truly precise measurements of the range difference between the spacecraft and two highly distant DSN stations.

A change of approach was clearly needed. The VLBI system was routinely measuring positions of extragalactic objects by directly measuring their signals' arrival time difference to the two stations involved. Unlike Doppler, this single measurement type could determine both right ascension and declination across the spectrum of nominal declinations. If differenced range was the object, rather than absolute range, couldn't a scheme be devised to perform the analogous operation on a signal originating directly from the spacecraft?

The stage was set to create a differenced one-way ranging data type and with it, the notion that these data and VLBI data could then be intertwined, thus merging the separate systems into a single, more powerful one. This unified system — code-named Δ DOR (delta-differential one-way ranging) — has matured into the DSN's most accurate system for precise planetary navigation. It is a highly operational system that can reliably produce results with accuracies approaching one nanoradian.

II. Beginnings: Reliance on Doppler Data for Planetary Navigation

From its earliest days, the DSN produced accurate Doppler data that was highly successful in determining the spacecraft orbit, whether the mission was lunar or planetary or whether the mission phase was cruise, encounter, orbiter, or landed. This article will concentrate on the cruise and preparation for encounter phases, historically the most important and difficult to determine well. Hamilton and Melbourne [5] first published the clear articulation of how Doppler data extracted the pertinent information to do this. There have been many elaborations and restatements of this seminal work, but briefly, it was noticed that to a good first approximation, a pass of Doppler data would behave as

$$\dot{\rho}(t) = \nu_r + \omega r_s \cos \delta \sin(\omega t + \Delta\lambda - \Delta\alpha) + n(t), \quad (1)$$

where

² VLBI was also being developed for the JPL Earth Physics Program: see Section III.

- $\dot{\rho}$ = Doppler observable of topocentric station–spacecraft range rate,
- ν_r = geocentric Earth–spacecraft range rate,
- ω = rotational velocity of Earth,
- r_s = distance of the tracking station from Earth’s spin axis,
- δ = nominal declination of the probe,
- $\Delta\alpha$ = difference between nominal probe right ascension and its actual value,
- $\Delta\lambda$ = difference between nominal station longitude and its actual value,
- $n(t)$ = noise on the data, usually modeled as random but in fact principally a convolution of various error sources affecting the data,
- $t = 0$ is chosen so as to place the nominal station just crossing underneath the nominal spacecraft position at epoch.

Thus, when tracking the probe with Doppler data, one would see the spacecraft’s geocentric range rate, but this value would have superimposed on it a diurnal modulation whose amplitude was a function of the spacecraft declination and whose phase was determined by the spacecraft right ascension. In addition, the dependence of this signature on the station location’s two primary components was explicit and inseparable from the spacecraft’s location. In other words, you had to know where the stations were in order to determine spacecraft position; errors in those components would lead to errors in the estimated position.

The role that the ranging system played was more of a boutique one at first. It was helpful when available — having a way to “scale” the otherwise angular measurements was very analogous to what the planetary ranging system did for the AU. But in fact, long arcs of Doppler data could fill out the missing parameters and determine the scale of things after only a few days.

An example of the specialized roles that the ranging system filled was in the improvement of the planetary ephemeris. Once a spacecraft is in planetary orbit, Doppler data alone can easily determine the spacecraft orbit relative to the planet. And once that is determined, ranging to the spacecraft can then supply a very accurate measure of the Earth–planet distance, contributing to the refinement of that planet’s ephemeris.

But Doppler was the workhorse. There were two fundamental reasons for this: precision and coherence. We have always spoken of Doppler as a measurement of velocity, but strictly speaking, the measurement is one of range change — the measurement appears as the integral of received frequency. And the measurement of this quantity has precision equal to the difference of the phase tracking at the beginning of the pass to perhaps the end. The precision of this measurement is on the order of a degree of radio frequency (RF) phase, less than a millimeter. That is not to say how accurate it is or was; both range and Doppler were vulnerable to much the same error set: charged-particle errors from both the ionosphere and space plasma, troposphere, drift in the station and spacecraft instrument calibrations and others. But the Doppler precision made these errors much more visible and ultimately helped in their calibration.

A single example may serve to clarify this point. It was long recognized that one of the ways to calibrate for charged-particle errors was to capitalize on the phenomenon that since range was a group phenomenon and Doppler a phase effect, charged particles would retard the former and advance the latter. So a measure of the charged-particle content was to accumulate differenced range vs. integrated Doppler (DRVID), and this number would be a measure of the change in the total number of electrons during the accumulation period [8]. Not bad, but the problem was that differencing the imprecise ranging measurements added lots of noise to the calibrations compared to the basic precision of the Doppler. And once a dual-band downlink was available, it was possible to calibrate the downlink very precisely with Doppler data alone; since the charged-particle effect went down by the square of the wavelength, the difference between the S- and X-band range change was indeed a measure of the charged-particle effect and one that preserved fully the high precision of the Doppler.³

The second key attribute was the coherence of both the range and the Doppler data. That the measurements were two-way in character greatly diminished the effects of timing and frequency errors, an otherwise dominant effect, particularly during the early era of rubidium standards used as the stations' clocks.

Consider the basic two-way operation: a state-of-the-art stable oscillator was used at the station to generate the uplink carrier, and the spacecraft received this signal, tracked it with a phase-locked loop, and used the newly derived signal as the reference for the downlink return — the frequency might be coherently multiplied to achieve separation from the uplink, or later, even shifted from S-band receive to X-band transmit, but the source of this transmission was a clean version of, and coherent with, the uplink itself.

When the return signal reached the ground station, a similar operation took place and a reference return signal was generated with a second phase-locked loop. This in turn was differenced with the uplink clock and the Doppler signal sent to a counter (Figure 1). Thus, the received signal was a copy of that originally sent, time-shifted, and modified only by any intervening media errors and the Doppler itself, the desired measurement. This scheme was remarkably insensitive to frequency and timing errors. For example:

- *Clock offset error.* This would amount to a time-tag error in the measurement and would show up as an error in UT (rotational position of Earth). In effect, the orbit produced would be “rotated” in right ascension by the amount Earth rotated during such a timing error; i.e., a microsecond clock error would produce less than 10 picoradians orbit error.
- *Clock rate offset.* Since all Doppler would be derived from the original frequency, the bias, or rate error, would manifest only as a slight proportional error in the wavelength and an error in the observed range rate by this measure. A typical offset in the rubidium clocks then used

$$\frac{\Delta f}{f} = 1 * 10^{-12}$$

³ A drawback to this later technique was that it did not directly measure the uplink so that the calibration of the downlink did not directly measure that component; many techniques were devised to infer the missing link from a series of the precise downlink measurements.

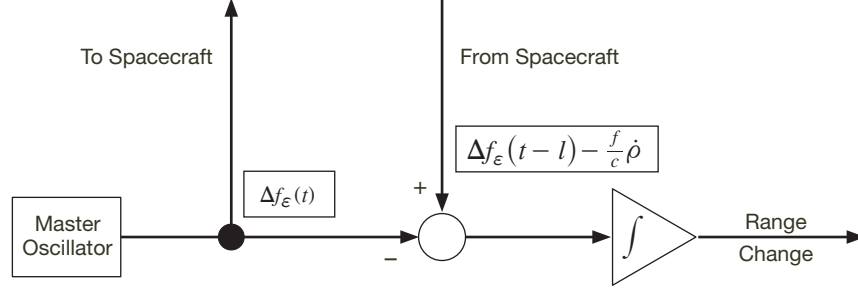


Figure 1. Conceptual block diagram for the coherent Doppler system.

and the measured range-rate error in a 10-km/s basic measurement would be only a few millimicrometers/s.

- *Clock drift.* This got all the attention since a drift during the round-trip light time (RTLT) would show up directly as a Doppler error, one for one. Here a drift, again of 1×10^{-12} , would appear as a Doppler measurement of

$$\frac{\Delta f_{\epsilon}}{f}c = 0.3 \text{ mm/s}.$$

As remarked just above, although the Doppler observable was always spoken of as velocity, the real observable was the integral of that velocity, or range change, and this was allowed to accumulate throughout the pass. The above error, if allowed to accumulate for say, 10 hr, would grow to 11 m, enough to destroy the data type's basic accuracy (the typical quote for Doppler accuracy of 1 mm/s was for random noise and propagated as the root of the pass length to 1.5 m — it was never an accurate compilation of residual error but was adjusted to be commensurate with what the errors measured in range change were thought to be). But even here, the properties of coherence intervened to limit the buildup of this error. Note that when passes are long and RTLTs are short — lunar and terrestrial planet missions never exceed 40 min and are usually much shorter — any error in the transmitted frequency, Δf_{ϵ} , would be sent to the integrator of Figure 1, starting to accumulate that massive range change already quoted. But one RTLT later, that same drift would return from the spacecraft and would reenter the integrator with opposite sign and would thus get removed. Viewed in this way, the accumulated range error can be written

$$\Delta \rho_{\epsilon} = -\frac{c}{f} \int_0^T \Delta f_{\epsilon}(t) - \Delta f_{\epsilon}(t-l) dt = -\frac{c}{f} \int_{T-l}^T \Delta f_{\epsilon}(t) dt + \frac{c}{f} \int_{-l}^0 \Delta f_{\epsilon}(t) dt, \quad (2)$$

where l is the RTLT, c is light speed, and T is the pass length.

For the restricted (but dominant) case of a slowly varying Δf_{ϵ} , this can be approximated as

$$\Delta \rho_{\epsilon} \approx -lc \left[\frac{\Delta f_{\epsilon}(T) - \Delta f_{\epsilon}(0)}{f} \right] \quad (3)$$

and the apparent runaway error from $\frac{\Delta f_{\epsilon}}{f} = 10^{-12}$ of 11 m would be held to 0.7 m — and much less for more typical l 's of, say, 15 min.

A similarly compelling case can be built for the coherent ranging system. Insensitivity to clock synchronization and rate offsets, and again, drift during the signal light time, introduced errors of under a meter.

But take away that coherence for either data type and the error budgets would have been completely dominated by clock-error effects. Coherence was seen as not only important, but absolutely essential; the range of options open to system developers did not realistically include noncoherent, one-way, data types.

Two-way Doppler was king, but a king with an Achilles' heel. It performed poorly near zero declination and, as was outlined in Section I, this was to be the case at the all-important Saturn encounter for the Voyager mission. So, for the first time in an important mission in a critical phase, the main role of determining declination, δ , was assigned to the ranging system and the mode required was to obtain nearly simultaneous ranging data from both the Goldstone, California, and the Canberra, Australia, complexes.

The geometry being used for such a data type is shown in Figure 2. Here, each station makes a two-way ranging acquisition with the spacecraft as shown. The difference in these two measurements (adjusted for the slightly different measurement times) is $B \sin \delta$. In the figure, the baseline is strictly north-south (NS), but the Goldstone-Canberra baseline contains a ~7300-km NS component adequate for determining the key declination component when that declination is unfavorable for Doppler determination. Figure 3 is copied from the Voyager navigation requirements document⁴ and serves to summarize the navigation accuracies that could be achieved circa 1975.

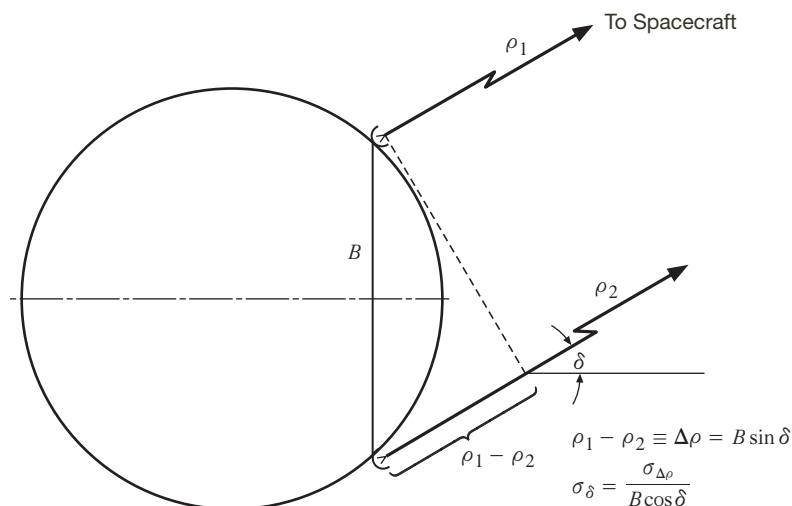


Figure 2. Geometry for nearly simultaneous differenced range.

⁴ D. W. Curkendall, editor, *Mariner Jupiter/Saturn 1977 Navigation Plan*, JPL Project Document 618-115 (internal document), Jet Propulsion Laboratory, Pasadena, California, December 1974.

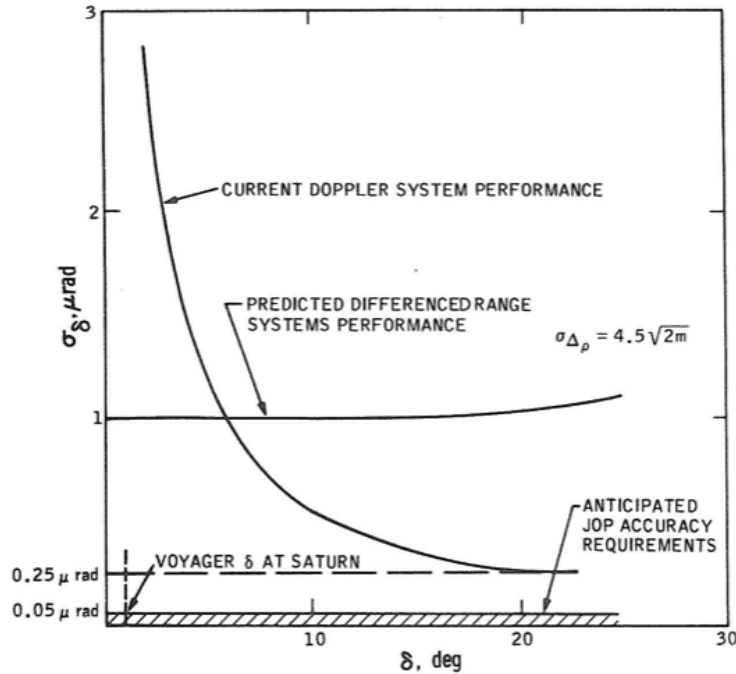


Figure 3. Accuracy plot from 1974 Voyager navigation requirements document.

As shown, for favorable geometries, declination (not shown, but right ascension as well) could be determined to approximately $0.25 \mu\text{rad}$ with gradually diminishing declination accuracy at the lower declinations. At the same time, the approximate 5-m ranging capability, if achieved, would stopgap this deterioration at about $1 \mu\text{rad}$. This accuracy was marginally adequate for Voyager and it was hard to see how this performance could be significantly improved. In truth, the ranging system was having trouble meeting these specifications and would have to go through an overhaul — changing from a square-wave ranging code modulation at 0.5 MHz to a series of pure sine waves topping at 1 MHz — to actually perform to this level. But from a longer-range perspective, the problem was that with only a 1-MHz ranging bandwidth to work with, really high precision was not going to be possible.⁵ To underscore these inadequacies, Figure 3 adds a future requirement for Jupiter Orbiter/Probe (JOP) — later named Galileo — at the $0.05\text{-}\mu\text{rad}$ level, to support a planned close flyby of Mars, that was far beyond what the differenced range could achieve.

III. Enter Very Long Baseline Interferometry

Developing in parallel with the spacecraft radiometric system was the rapid implementation of the technology to perform VLBI. Unlike the planetary navigation system, which was unique to JPL, VLBI enjoyed a national constituency of several cooperating and competing centers. Principal among these were the consortium at Massachusetts Institute of Technology led by Irwin Shapiro, Chuck Counselman, and Alan Rogers [9] and a very active group at NASA's Goddard Space Flight Center led by Tom Clark [10]. The JPL group was first led

⁵ The problem here was that it was difficult (and still is) to handle wide bandwidths through the demodulation process in the spacecraft uplink receiver. In 2010, the highest ranging tone was still at 1 MHz.

by Jack Fanelow [11]. Further, since VLBI depended on widely distributed antennas, a burgeoning international community had also formed with many centers springing up wherever suitable observational sites and associated baselines existed. There were many engineering and scientific goals of these enterprises: radio source catalog development, astrometric positions and source structure, measurement of Earth’s dynamic parameters such as UT and PM, and the measurement of intercontinental drift were prime examples.

Since there was no coherence in this measurement strategy, unlike the two-way Doppler and range we have been describing, most efforts included at least an R&D hydrogen maser as the station’s master clock. The two and then three orders of magnitude greater stability promised and then demonstrated by these devices was to prove to be the “Mother’s Milk”⁶ of VLBI; and by extension it was to prove the same for the eventual DSN evolution to non-coherent radiometric measurement systems. More than any other component, it was the element most important in enabling the migration to one-way data and Δ DOR, the main subject of this article. Experimental hydrogen masers had been in use since circa 1970, and by 1977 Richard Sydnor was building operational masers for the DSN and reporting stabilities of a few parts in 10^{-15} over 1000 s and beyond [12].

VLBI was completely devoted to measuring that range difference, as is depicted in Figure 2 (wideband data) and to its change (narrowband data). Of the two, the former was to prove by far the more productive.

There are many references and tutorials on VLBI basics [13–16], but briefly, the VLBI process records multiple channels (typically 2 MHz in width) onto tapes (now onto disks) at each of two (or more) stations observing an extragalactic radio source (EGRS). Later, the two tapes are brought to a single location and are cross-correlated, looking for the time delay (tape shift) that is needed to just align the two recordings — since the EGRS is distant, its radio waves will be plane waves and identical signals will reach both stations but with a time difference that can measure the range difference (as in Figure 2). The cross-correlation function of the two signals can be shown to be

$$R(\Delta\tau) = KW \frac{\sin(\pi W \Delta\tau)}{\pi W \Delta\tau} \cos(2\pi f_c \Delta\tau), \quad (4)$$

where

$\Delta\tau$ = the misalignment of the two tapes from the actual time delay, i.e.,
the two signals will exactly line up when $\Delta\tau$ is zero,

W = channel bandwidth (e.g., 2 MHz),

f_c = RF center frequency of the channel,

K = system gain factor.

That is, this correlation function consists of two parts:

⁶ A favorite phrase of Pete MacDoran in promoting the importance of the hydrogen maser.

- (i) The correlation magnitude, a slowly varying function of $\Delta\tau$, in this instance first falling to zero at $\Delta\tau = W^{-1}$ or $0.5 \mu\text{s}$ — about 150 m in range difference,
- (ii) The rapidly varying part, or fast fringes, the cosine function in Equation (4).

The magnitude portion of Equation (4) is too broad to find the $\Delta\tau = 0$ point precisely. The cosine portion must also be employed, and indeed the delay necessary to zero the cosine function can be determined to a few degrees of an RF cycle. The problem with that is that it is periodic in one cycle of RF and it is in general impossible to tell which of those cycles corresponds to the coincident peak of the magnitude portion.

To resolve this ambiguity, we can record at least one more 2-MHz channel at, let's say for specificity, 10 MHz distant from the first. If we do a cross-correlation on this channel and use exactly the same trial tape shift, we can again measure the phase of the cosine and will find it has shifted slightly in accordance with

$$\frac{\partial\Delta\phi}{\partial f} = 2\pi \frac{\Delta\rho}{c}.$$

The phase shift, $\Delta\phi$, will be equal to

$$\Delta\phi = 2\pi \frac{\Delta\rho}{c} [f_{c1} - f_{c2}], \quad (5)$$

or, rearranging,

$$\Delta\rho = \frac{c\Delta\phi}{2\pi[f_{c1} - f_{c2}]} \quad (6)$$

The ambiguities are still there, but the wavelength of the frequency difference — 10 MHz — is now 30 m, not the 3.6 cm of the DSN's X-band. If we know the range difference a priori to under 30 m — remember that this would be equivalent to knowing a priori the source position to maybe $2 \mu\text{rad}$, a modest initial requirement — we can then have an unambiguous measurement of that parameter. Of course, it is not as precise as that that could be given with the single channel. Our precision has suffered by the same 8,400/10 ratio.

But with several of these channels, judiciously spaced, we can work our way up from what we do know to the precision enabled by the most highly separated channels. From the beginning, a 40-MHz spanned bandwidth was typical in the receiver implementations for all the North American VLBI participants, a spanned bandwidth that permitted the measurement precision to be under 2 cm. This process, known as bandwidth synthesis, was first proposed by Alan Rogers [17].

This VLBI scheme was at its heart quite analogous to the spacecraft navigation problem in that it was attempting to measure the astrometric positions of, in this instance, the EGRSs. But it enjoyed several advantages:

- Its wideband mode operated at 40 MHz, instead of the 0.5 to 1 MHz of the two-way ranging system.

- The proper motion of the EGRS was zero. Once one determined the astrometric position of it, it stayed fixed. And multiple stations with multiple baselines could be used in that determination, averaging and minimizing the effects of station-location errors of any one.
- And with an accurate source catalog, it could then be used in reverse to determine those station-location errors and monitor the variations in UT and PM.
- The data were one-way and hence subject to clock-error effects that we have been discussing, but with the advent of the hydrogen masers, these were controllable and clock offset and rate could be observable during a long VLBI session, solved for, and largely removed.

This same VLBI community was not unaware that the VLBI infrastructure might be leveraged to include spacecraft in their source lists and in effect perform Δ VLBI — i.e., measure the spacecraft position relative to an EGRS [18]. Early attempts by Slade [19] sought to use narrowband Δ VLBI to track the Mars-orbiting Mariner 9 and hence relate the planet to the quasar frame. These early attempts were hampered by immature station instrumentation and signal-processing difficulties, though a planetary–quasar frame tie was finally established at the 100-nrad level [20]. We quote from Border [21]:

The earliest measurements, begun in 1972 with the Mariner 9 spacecraft in orbit at Mars, proved difficult. These measurements had the dual purpose of developing the VLBI technique in the DSN while also measuring the position of Mars in the radio reference frame. But problems were encountered with station instrumentation, specifically with frequency stability in the signal downconversion chain needed to capture the spacecraft signal in the video (baseband) channel of the VLBI recorder. Also, media effects were large at the frequency of the S-band downlink and new algorithms had to be developed for processing spacecraft signals since their spectral characteristics differed from those of natural radio sources. Ultimately, it would take years before high-quality results were obtained. Over this time, DSN instrumentation was improved to meet the demands of the new VLBI program as well as to better serve other users.

...

Efforts continued to make Delta-VLBI phase delay rate observations of the Viking orbiters at Mars and the Pioneer 12 orbiter at Venus. Between 1980 and 1983, eight successful passes were made with Viking and three successful passes were made with Pioneer 12, all with dual-band S/X downlinks. All these data were combined to estimate a rotational offset between the radio frame and the frame of the inner planets. An accuracy of about 100 nrad was achieved for both right ascension and declination components with the limiting error source being knowledge of the spacecraft orbits relative to the planet centers.

Technologists from the spacecraft navigation community grew interested. In 1977, Miller and Rourke [22] performed an accuracy analysis study that showed that if measurements could be taken with high accuracy relative to a quasar during a Jupiter approach, one could determine the Jupiter relative orbit with only loose a priori knowledge of the planet's ephemeris. The charting of Jupiter's gravitational effect on the trajectory would disclose the planet's position.

But in general, these early proposals focused on cross-correlating the spacecraft signal as if it were a natural noise-generating source. Problems were inherent in this approach. The spacecraft signal is ever changing depending upon telemetry broadcasts, etc., and its bandwidth will vary greatly both from project to project and even mission phase. Finally, although the energy flux density from quasars is weak, it is still strong when compared to a spacecraft signal spread over several MHz.⁷ And cross-correlating the spacecraft signals inevitably brings the receiver noise from each station into multiplicative play. What was needed was a comprehensive approach to supply an appropriate spacecraft signal and a signal-processing scheme that tracked that signal from each station and without cross-correlation.

IV. Delta-DOR Is Formally Proposed

In 1977, Melbourne and Curkendall [23] published a comprehensive outline proposing a Δ DOR system that featured a custom signal generator on board the spacecraft that created a waveform that could be used to determine one-way range, and specifically the difference in one-way range, to each of two or more target stations. The signal structure adopted was to mirror closely the recorded bands of the VLBI quasar receptions. Referring to Figure 4, the DOR spacecraft transponder modulates the carrier with a series of pure tones of escalating frequency relative to the carrier. The signals received at the stations are sent through the open-loop VLBI receivers, recorded, and phase-tracked in postprocessing.

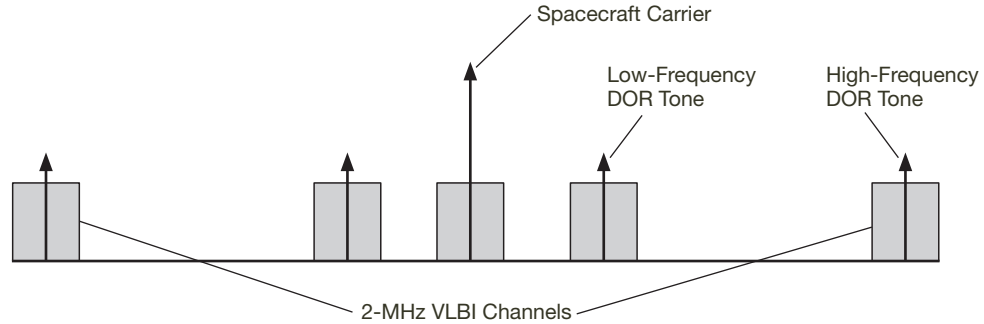


Figure 4. Downlink tones strategically placed and showing coincident VLBI channels.

The determination of range and range difference proceeds exactly as in the previous section, except that each recording is individually tracked to determine individual phase so that cross-correlation need never take place. For each tone, a phase is determined relative to a specific epoch at each station and then differenced to obtain a measure of the range difference. This phase difference is ambiguous to within an RF cycle, i.e.,

$$\Delta\rho = \frac{(\Delta\phi + 2\pi n)c}{2\pi f_1}, \quad (7)$$

⁷ The signal flux density of a typical quasar observed for Δ DOR is 0.5 Jy, where 1 Jy = 10^{-26} W/m²/Hz. The received power-to-noise spectral density ratio of a typical spacecraft ranging code is 20 dB • Hz at a DSN 34-m antenna, corresponding to a signal flux of 7.6×10^{-23} W/m². If viewed as flux density over a 2-MHz channel bandwidth, the spacecraft signal flux density is 0.004 Jy.

where n is an unknown integer. But, as in the VLBI case,

$$\frac{\Delta\Delta\phi}{\Delta f} = 2\pi \frac{\Delta\rho}{c} \quad (8)$$

and we can measure the change — $\Delta\Delta\phi$ — in the phase difference at two frequencies and obtain a lower precision estimate just as in the VLBI case (cf. Equation [6]). In this way, the range difference can be roughed-in via the low-frequency tones and made precise with the outer pair shown in Figure 4. From the onset, the goal was to have the highest spanned bandwidth to be on the order of 40 MHz, and, as we shall see in the next section, is now often as high as 76 MHz. And at these frequencies, the wavelength — whose phase can be measured to on the order of a degree — gives a fundamental path-delay measuring ability approaching a single centimeter.

This procedure is referred to as DOR — differential one-way range. As compared to the more conventional coherent data types, it is dramatically more sensitive to station clock offsets and drift as was discussed earlier, has decreased sensitivity to interplanetary plasma effects, and has similar behavior with respect to station-location errors — including UT and PM — and local troposphere and ionospheric disturbances. In the pure DOR mode, it was planned to operate the VLBI system alongside the spacecraft radiometric system and provide calibrations for clock offsets and for variations in UT/PM.

Figure 5 shows the basic geometry as seen from both equatorial and polar projections. From an information content point of view, it is easily derived that this observable is related to spacecraft position and platform parameters as

$$\Delta\rho = B_E \cos \delta \sin(\omega t + \Delta\lambda - \Delta\alpha) + B_z \sin \delta, \quad (9)$$

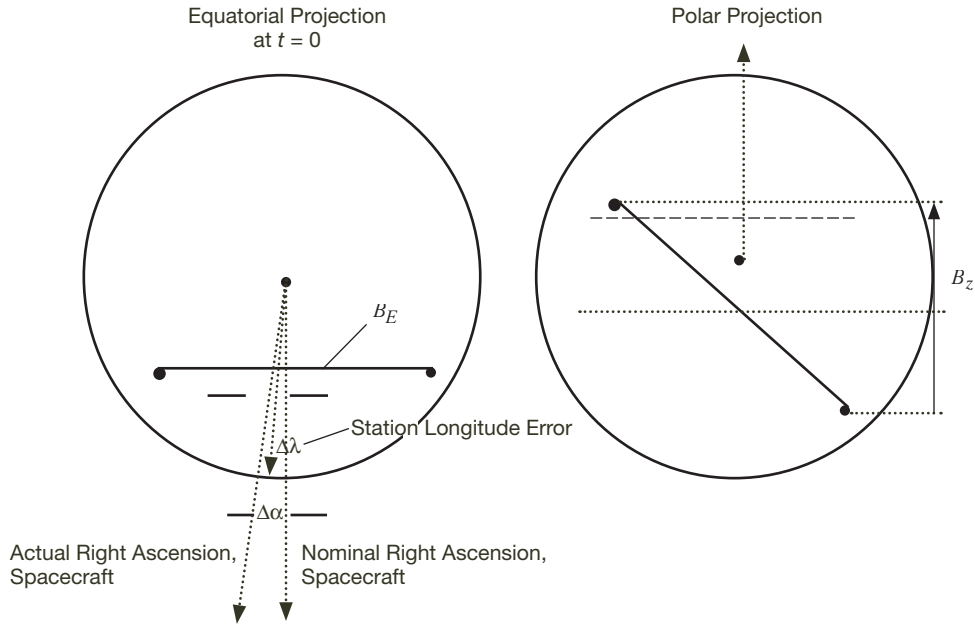


Figure 5. Geometric depiction of terms in Equation (9) at nominal meridian crossing.

where

- B_E is the equatorial projection of the baseline linking the two stations,
- B_z is the polar projection of that same baseline,
- δ is the spacecraft declination,
- $\Delta\alpha$ is the difference in right ascension between the nominal spacecraft right ascension and its actual value,
- $\Delta\lambda$ is the station-location error in the longitude component,
- ω is the Earth rotation rate,
- t is measured from when the nominal right ascension is at a value that places the spacecraft at high noon with respect to the equatorial baseline.

Note that the five relevant partials

$$\begin{aligned}\frac{\partial\Delta\rho}{\partial\Delta\alpha} &= -B_E \cos\delta \cos(\omega t) \\ \frac{\partial\Delta\rho}{\partial\delta} &= -B_E \sin\delta \sin(\omega t) + B_z \cos\delta \\ \frac{\partial\Delta\rho}{\partial\Delta\lambda} &= B_E \cos\delta \cos(\omega t) \\ \frac{\partial\Delta\rho}{\partial B_E} &= \cos\delta \sin(\omega t) \\ \frac{\partial\Delta\rho}{\partial B_z} &= \sin\delta\end{aligned}$$

disclose that over any one pass, station longitude and right ascension alias for one another and cannot be separated, whereas B_E and B_z each have unique signatures and are weakly separable from the two spacecraft parameters. In practice, since the overlaps in the station passes are short for the desired intercontinental baselines, any attempt at a combined solution would be very weak and is never mounted. What is effective is that the international effort that builds the EGRS catalogs can observe the quasars from many baselines — sometimes as many as 20 stations and more than 190 baselines are used in a single solution, as is discussed by Ma [24]. In total, in the calculation of EGRS position, this multiplicity averages down the contribution from any one set of baseline errors to arrive at a solution for EGRS position much better than can be obtained from a single baseline. Once those astrometric positions have been established, an observation of one or more of these accurately positioned EGRSs from any desired baseline pair can be used to refine that baseline estimate in this self-referential manner.

These better solutions are useful, but in practice, are not used in the stand-alone mode of measuring $\Delta\rho$ of the spacecraft coupled with a separate VLBI pass to calibrate for UT/PM and clock effects. Instead, the spacecraft is always observed in an interlocking back-and-forth pass of both an angularly nearby quasar and the spacecraft itself. DOR becomes Δ DOR, where the Delta prefix refers to one more differencing operation with a nearby EGRS. That is, the real observable becomes

$$\tau_S - \tau_Q,$$

where the two τ 's measure the two-station time delay differences of the spacecraft (S) and the quasar (Q), respectively. Here, we have dropped the explicit references to range difference and adopted the current usage of expressing the observable in the time domain, but they are related as in $\tau = \Delta\rho/c$. We will denote total measured time delays by τ , and the difference between measured delay and nominal delay by $\Delta\tau$.

A pass of this type of data proceeds with both antennae trained first on the quasar and then back to the spacecraft with a dwell time of ~ 5 min/source. This repeats until the end of the pass.

With this last difference, Equation (9) is modified — adding the terms contributed by the EGRS — and is replaced by the difference between the (Earth-centric) spacecraft observation and the quasar observation itself. And note that since the quasar is angularly close by the spacecraft, the quasar and spacecraft terms are nearly identical in their numerical evaluation. The process, then, models the positions of both objects as carefully as possible and takes that model out of the observables, leaving the difference between the residuals of these two objects. And this, of course has the dramatic effect of differencing out common mode errors — discussed separately just below — and, in essence tying the estimate of the spacecraft position closely to that of the quasar.

Imagine for the moment that we use these residuals to form an estimate of just the spacecraft position while leaving the coordinates of the EGRS fixed. In linear form, then, we have the basic normal equations to invert, but in this case, the parameters being determined will be restricted to the spacecraft coordinates; the effect of the quasar partials (and residuals) will simply be absorbed in this estimate. We have

$$z = [\Delta\tau_S - \Delta\tau_Q] = A \begin{bmatrix} \Delta\alpha \\ \Delta\delta \end{bmatrix}_S - B \begin{bmatrix} \Delta\alpha \\ \Delta\delta \end{bmatrix}_Q, \quad (10)$$

where the data vectors are the residuals from the best model. If we solve just for the spacecraft, we have

$$\begin{bmatrix} \hat{\Delta\alpha} \\ \hat{\Delta\delta} \end{bmatrix}_S = (A^T A)^{-1} (A^T A) \begin{bmatrix} \Delta\alpha \\ \Delta\delta \end{bmatrix}_S - (A^T A)^{-1} (A^T B) \begin{bmatrix} \hat{\Delta\alpha} \\ \hat{\Delta\delta} \end{bmatrix}_Q. \quad (11)$$

Since both the A and B partials are of the same form, $(A^T A)^{-1} (A^T B)$ becomes nearly the identity. And for the restricted case where the nominal positions of the two objects *are* the same (there is null angular separation between the bodies), it *is* the identity. In this case, Equation (11) becomes

$$\begin{bmatrix} \hat{\Delta\alpha} \\ \hat{\Delta\delta} \end{bmatrix}_S = \begin{bmatrix} \Delta\alpha \\ \Delta\delta \end{bmatrix}_S - \begin{bmatrix} \hat{\Delta\alpha} \\ \hat{\Delta\delta} \end{bmatrix}_Q + \text{noise}, \quad (12)$$

where the $\hat{}$ symbol denotes *estimate of* instead of the true value, without the $\hat{}$. In Equation (12), the $\hat{}$ over the quasar's coordinates implies we will use the catalog estimate of the quasar's position, not exposing it to update via the current data.

So, in this circumstance there is a one-to-one correspondence between a change in an EGRS catalog position and the corresponding change in the estimate for the spacecraft position (and in the general nonzero but small angular separation circumstance, this correspondence will be close). In other words, by this artifice, we are now navigating relative to the quasar frame.

The implications are profound in that we must now know the target ephemerides in that frame. These frame issues will be discussed in Section IX, but this re-referencing operation permits us to take advantage of both the radio character and the zero proper motion properties of these reference stars. And most importantly, it permits us to dramatically reduce the major error sources affecting the accuracy of a stand-alone measurement of $\Delta\tau_S$ by its difference with $\Delta\tau_Q$. This final difference contains all of the desired geometric information, but will common-mode out a large percentage of the stand-alone errors.

Finally, standard practice often enlists a second quasar into the sequence so that instead of QSQSQ.... as the sequence, we would have $Q_1 SQ_2 SQ_1$ The idea here is that by selecting a second radio source as equidistant as possible from the spacecraft (but on the other side of) as the first source, we create a virtual source closer to the spacecraft than would be otherwise possible. And by this measure, the degree of common-mode error cancellation increases (within the limits of linearity). This idea will be formally demonstrated in the following subsection.

Section VIII will quantify all the major errors sources for a typical Δ DOR measurement. Here, we will be content to illustrate just two: *platform inaccuracies* (station locations, etc.) and during the subsequent discussion of the data (Section V), *clock effects*.

Platform Errors. Imagine the situation as depicted in Figure 6, which shows a typical dual measurement of first a spacecraft and then of an EGRS. Imagine further the baseline errors, $\vec{\Delta B}$, are a random and spherically distributed variable as shown. It is clear that the contribution to the measurement error from a station-location error is

$$\begin{aligned}\epsilon_{\tau_S} &= \vec{\Delta B} \cdot \hat{S}_S \\ \text{and} \\ \epsilon_{\tau_Q} &= \vec{\Delta B} \cdot \hat{S}_Q.\end{aligned}\tag{13}$$

That is, the error in the measurement is simply the component of the station-location error in the spacecraft (or quasar) line of sight. These of course are similar, but different. If we difference the two measurements, the residual error will be

$$\epsilon_{\tau_S} - \epsilon_{\tau_Q} = \vec{\Delta B} \cdot (\hat{S}_S - \hat{S}_Q) = \vec{\Delta B} \cdot \hat{S}_{S-Q} = |\vec{\Delta B}| \theta.\tag{14}$$

Figure 6 details the meaning of the symbols in Equations (13) and (14), but briefly,

$\vec{\Delta B}$ is the assumed spherically distributed baseline error, which can conceptually also contain uncalibrated UT/PM,

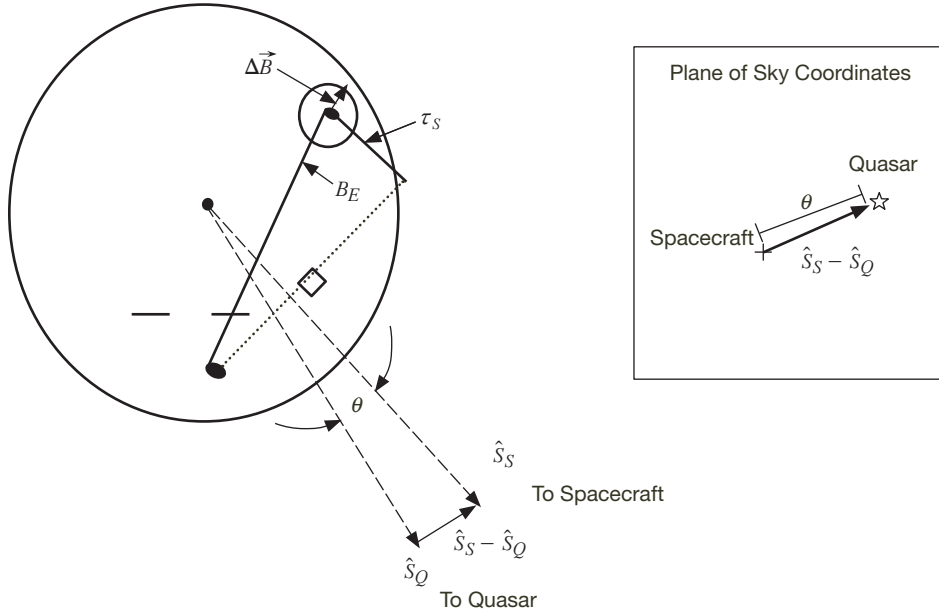


Figure 6. Basic geometry and some definitions for Δ DOR measurements.

\hat{S}_S, \hat{S}_Q are the unit Earth spacecraft and quasar vectors,

θ is the angular distance from quasar to spacecraft in plane-of-sky (POS) coordinates.

Note that the expected error reduces down by this angle, θ , which, say, for 6 deg would reduce the root-mean-square (rms) errors down to less than 10 percent of their unreduced amplitude. Note also that the direction of the error's contribution changes from the line of sight to perpendicular to that and in the direction of the difference of the two line-of-sight vectors, as shown in the POS inset drawing of Figure 6. So, the strategy is to get the best solutions possible for station locations and for UT/PM and then reduce those further by up to an order of magnitude by the final differencing operation.

In the case where we have two quasars and we will average their (residual) time delays before differencing, not much changes; we have

$$\left[\Delta\tau_S - \frac{\Delta\tau_{Q1} + \Delta\tau_{Q2}}{2} \right]. \quad (15)$$

And in this case, continuing on in parallel with the single-quasar case just above, the three measurement errors from platform errors contain a modified term (see vector and POS sketch in Figure 7):

$$\epsilon_{\tau_{Q1SQ2}} = \Delta\vec{B} \cdot \left[\hat{S}_S - \frac{\hat{S}_{Q1} + \hat{S}_{Q2}}{2} \right] \quad (16)$$

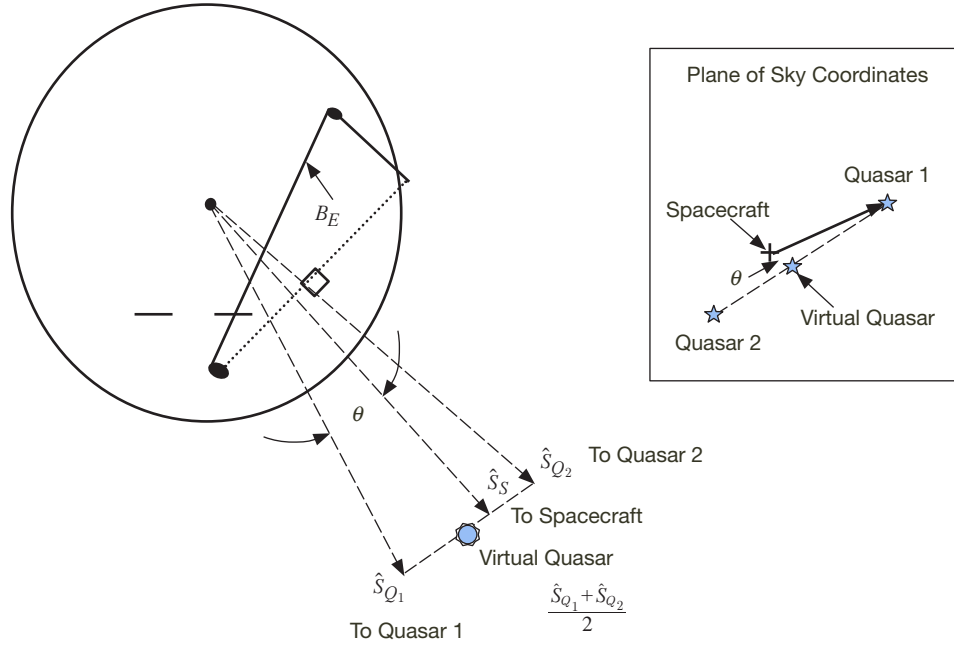


Figure 7. Best practice seeks to use two quasars bracketing the spacecraft in the POS.

As Equation (16) details, the measurement is, not surprisingly, as if from a single virtual source halfway between the two. This two-EGRS strategy is often very helpful at creating virtual geometries with lower error source sensitivities than from any of the actual single sources available. The sensitivities from this virtual source (within the limits of linearity) will be the same as in Equation (14), except that the quasar is replaced by a virtual one just halfway between the two originals.

Platform parameters today are easily known to the few-cm level, so remaining effects for Δ DOR measurements, after differencing, are sub-cm. Similarly, media delays for a single line of sight may usually be calibrated to the 10-cm level or better, again leaving only cm-level errors for Δ DOR measurements. And it was noted earlier that measurement precision for the available 40-MHz spanned bandwidth approaches the cm level. A full error budget is given in Section VIII. Note that 1-cm uncertainty in path delay corresponds to 0.033-ns uncertainty in measurement of time delay, and this in turn corresponds to approximately 1.25-nrad angular uncertainty for measurements on DSN intercontinental baselines. Indeed, measurement accuracy today approaches 1 nrad for favorable geometries that include observations at higher elevation angles and close proximity to a strong radio source, while accuracy of 2 nrad can be obtained for most actual geometries encountered during flight operations.

V. The Data

We start by discussing recent data that are of the highest quality. The plot shown in Figure 8 represents a pass approximately 5000 s in duration — of *differential* delay data between stations DSS-26 and DSS-43 (Goldstone–Canberra). The data were obtained from

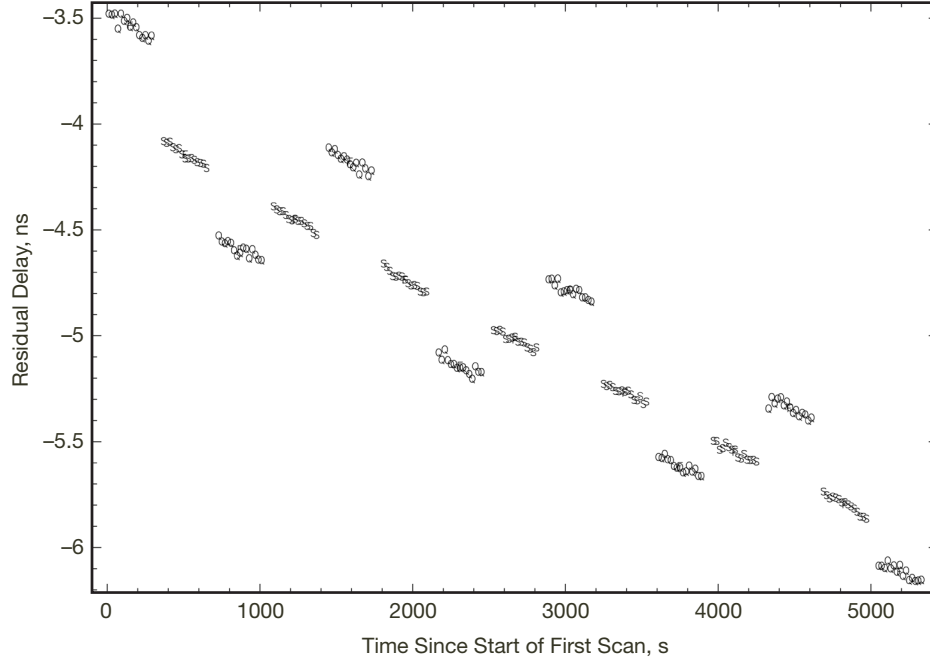


Figure 8. An MRO in-orbit pass of Δ DOR data involving two quasars.

the Mars Reconnaissance Orbiter (MRO) while it was in Mars orbit. There are three time series of data shown here: from the spacecraft itself shown as the middle track (denoted as “S”) and, in this case, from two nearby EGRSs (denoted as “Q”). There are individual delay measurements, about 20 per dwell time, and the antennae are slewed in a Q_1, S, Q_2, S, \dots sequence for a total of seven dwells on the spacecraft and four each on the EGRSs. There really are six such figures for this pass, one for each of the frequency separations, as is shown cryptically in Figure 4. We show only the widest frequency band, a 38.4-MHz DOR tone harmonic for a total spanned bandwidth of 76.7 MHz. As discussed above, the lower frequency tones are used for ambiguity resolution; the final measurements are taken only from the highest frequency tone spacing.

Each point, then, represents the delay calculated from phase difference as tracked by the tone tracker (spacecraft) or fringe-fitting software (quasar). Measured phase difference is converted to delay by dividing by the spanned bandwidth as in Equation (8). Next, ambiguities are removed at the wavelength of the 76-MHz tone. As part of the data validation and conditioning process, dwell length local fits (linear) are made to both the quasar dwells and the spacecraft dwells, compressing the delay measurements to one point per observation dwell time. These normal points — two quasar delays and one spacecraft delay for each QSQ sequence — are passed from the data measurement team function to the navigation team. It is important to realize that Figure 8 plots not the delay data as measured, but with relatively crude models of source positions, media effects, etc., backed out of the data so we have a readily interpreted display of the resulting residuals for data validation, and for now, elucidation. Once the models are removed, the delay data are as described via Equation (9).

Clock Effects. Note that the ultimate differencing operation eclipses the offset error in station clocks, but a main feature observed in Figure 8 is that the station-frequency offset contributes a major portion of the downward data slope. We had identified station clocks as

a main contributing error source for one-way data, and at first glance it appears that clock-frequency offset strongly affects the data. But this is the primary reason that observations are made in the quasar–spacecraft–quasar sequence. The interpolation of the quasar delays to the time of the spacecraft delay exactly removes the linear portion of the station-clock drift. Small deviations of the station-clock drift from linear are accounted for in the Δ DOR error budget. The use of highly stable hydrogen maser clocks keeps this error source small. Note that Figure 8 displays three distinct tracks offset from each other by about 0.5 ns (~ 15 cm). If the clock-frequency offset was all that was going on, these three tracks would all lie on a single straight line. That they are offset illustrates the effects of platform parameters and media effects that have not yet been accurately taken into account. But notice that if we replace the two quasars with the virtual one halfway in between by averaging these same delays, this third virtual track indeed lies very close to the spacecraft track itself.⁸ In this way, interpolation of quasar delays to the time of the spacecraft delay reduces spatial as well as temporal error sources. Differencing with nearby quasars is demonstrably beneficial and the closer the proximity, the better.

Model delay is restored by the data measurement team, and then total delay is delivered to the navigation team for each normal point. Thus, the observables do not depend on models or calibrations applied during data compression. The navigation team carefully calibrates the total delays for media and platform effects — using best available models [25] — and once again leaves residual delays. A single normal point of delay difference is calculated for each triplet of dwell times, and this is used in the final state estimate performed by the navigation team. Actually, Δ DOR data from Mars orbit are used to estimate the ephemeris of Mars rather than spacecraft state.

As explained in Section IX, data obtained from Mars orbit are indispensable for aligning the planetary ephemeris with the radio reference frame. But the primary use of Δ DOR is to support cruise navigation, in particular determining spacecraft angular position. Navigators then use this information to adjust the spacecraft course as needed to arrive at an intended target. Figure 9 shows Δ DOR residuals from early in the cruise phase of Mars 2001 Odyssey. Residuals are with respect to a trajectory that was determined from the first segment of data and then predicted forward. The residuals over the reconstructed portion of the trajectory are small and well-behaved, but the trajectory prediction is clearly in error. In fact, the residuals provide a direct estimate of the trajectory error. Two conclusions are evident. First, it is necessary to continue acquiring data in order to accurately determine the trajectory, and second, force models acting on the spacecraft need to be improved.

The Odyssey spacecraft was asymmetric and experienced a high level of solar torque. The prelaunch solar pressure and attitude control force models did not lead to good acceleration predictions for trajectory propagation. Force modeling was studied during early cruise, aided by the availability of accurate spacecraft position and velocity measurements. Improved models were developed, and a strategy was devised to reorient the spacecraft to minimize force model uncertainty.

⁸ The two quasars for this track lie 8.1 deg and 6.1 deg on either side of the spacecraft in POS coordinates. The *virtual* source lies 3.5 deg from the spacecraft, and as expected, the re-referencing operation brings the tracks into better coincidence, even before more carefully constructed models and calibrations are applied.

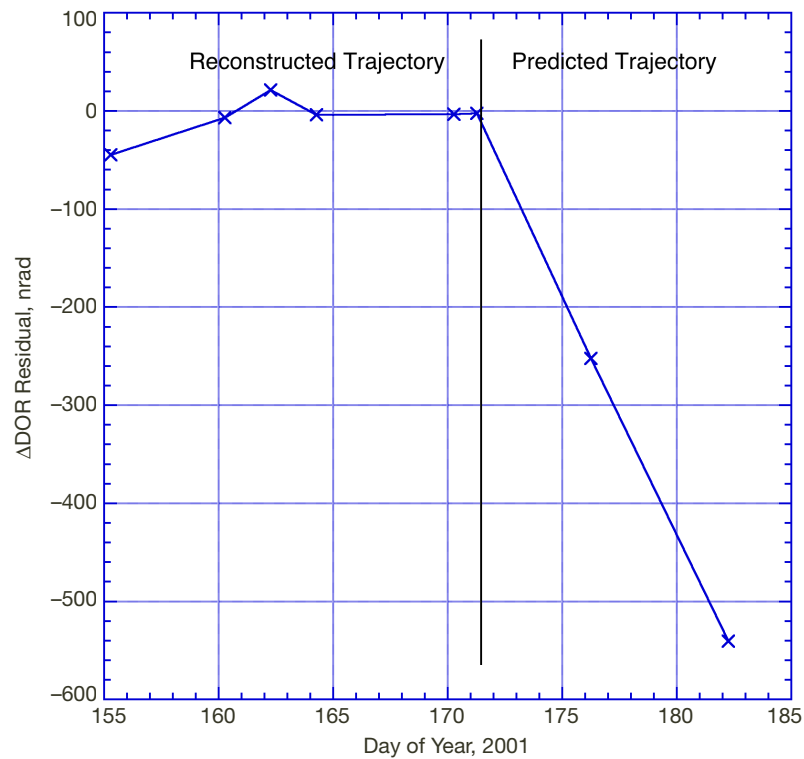


Figure 9. Early cruise Δ DOR residuals from Mars 2001 Odyssey.

At a given time during cruise, trajectory predictions extended to the target are used to assess how close or far the spacecraft would be from its target if no course adjustments were made. Typically, a few trajectory correction maneuvers are planned during cruise. Tracking data are acquired to first plan and then reconstruct each maneuver. Good tracking data allow for accurate maneuver design, and performing the larger maneuvers early in cruise is much more fuel efficient. As the spacecraft nears its target, data accuracy becomes even more decisive as prediction span decreases. Trajectory predictions for Odyssey were much more accurate later in cruise, Δ DOR data correctly measured spacecraft position, and the spacecraft arrived at Mars with unprecedented accuracy.

When planning Δ DOR support for a mission, the region along the trajectory is searched to identify radio sources that could be used as reference sources. Figure 10 shows the pre-launch planning cruise trajectory of Mars Science Laboratory (MSL) in POS coordinates, along with well-known radio sources from the quasar catalog.⁹ Additional candidate sources that have recently been added to the catalog are also shown. Different sources must be selected for observation as the spacecraft moves across the sky as seen from Earth. There is often a trade between selecting stronger sources at greater angular separation from the spacecraft, or weaker sources at smaller angular separation. To support navigation analyses, Δ DOR observations are tentatively planned for every measurement opportunity, i.e., one measurement per day per DSN baseline throughout cruise. An estimate of expected data accuracy is provided based on the spacecraft transmitter characteristics and the trajectory geometry. This allows detailed studies of predicted navigation delivery accuracy. Then the

⁹ This article was written before MSL launch.

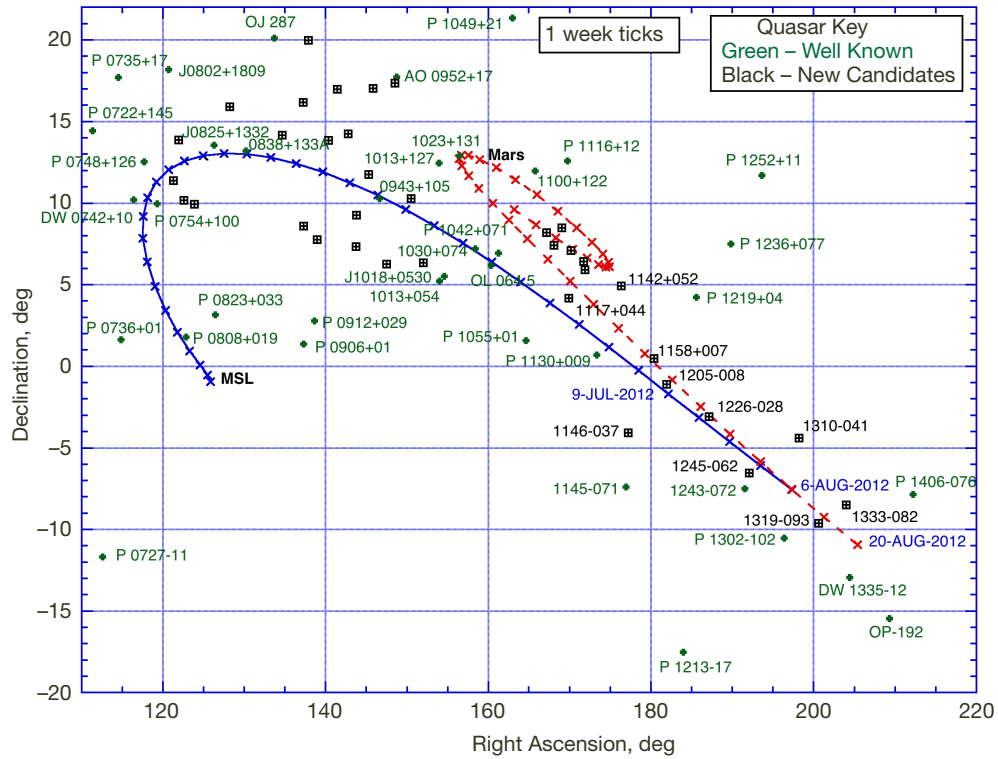


Figure 10. MSL prelaunch cruise trajectory showing both well-known and new candidate reference sources (some source names are not shown).

tentative schedule is updated as the reference trajectory is updated and as more survey data about candidate radio sources becomes available.

After data have been acquired over some time interval, accuracy can be assessed by examining measurement residuals. There were a total of 64 Δ DOR sessions using DSN antennas during the MRO cruise phase from Earth to Mars. One or two angularly nearby sources were selected for observation during any one session. Figure 11 displays the Δ DOR residuals with respect to the final reconstructed cruise trajectory. Each session has approximately 1 hr of data either on the Goldstone–Madrid or the Goldstone–Canberra baseline. Nine separate radio source dwells were made during each session, and hence three interpolated QSQ normal points were generated for each session. Note that there are neither trends nor significant biases remaining in these data and “system” noise measures 1.18 nrad (0.031 ns) rms, close to the expected level of accuracy. A summary of the final cruise navigation results is contained in Figure 12, republished from the JPL navigation team’s definitive description of the cruise and encounter phase navigation activities as reported by Tung-Han You [26].

Figure 12 displays the various orbit determination solutions as a function of the data types included using data up to Mars orbit insertion (MOI) minus 13 hr. The final navigation knowledge uncertainty (conservative) was determined to be about 0.4 km, 1 sigma. Note how the estimates converge to that finally approved estimate only when Δ DOR is included in the data set. Unlike flyby missions, there is no postconstruction of “ground truth” when the mission calls for a planet insertion deboost shortly after the final orbit is determined,

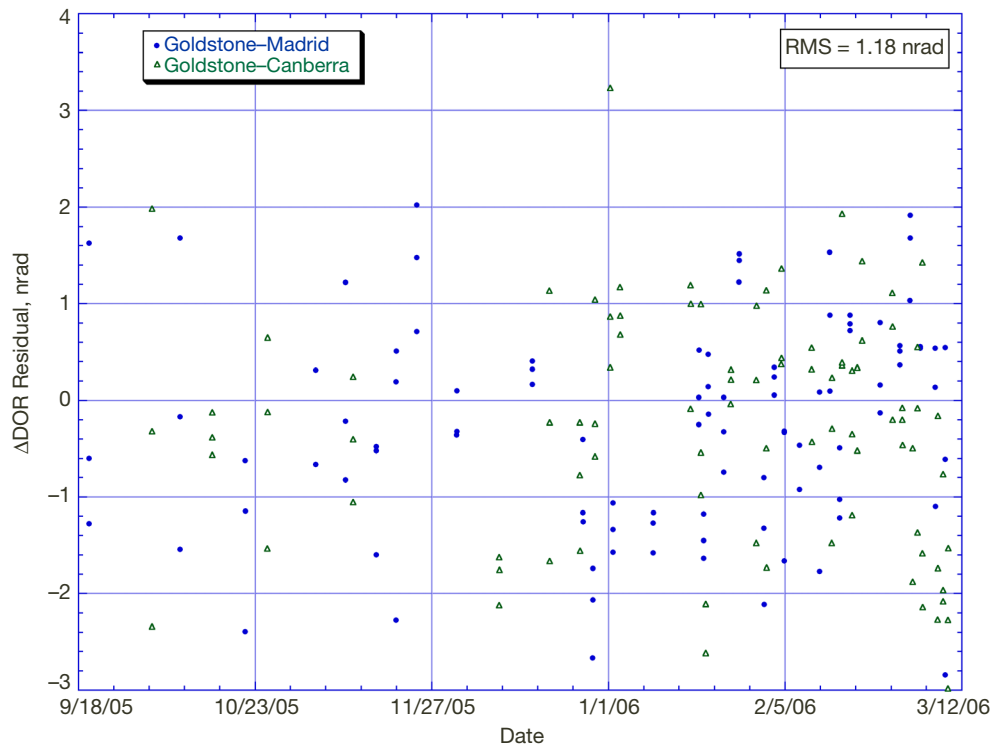


Figure 11. MRO Δ DOR residuals to final reconstructed cruise trajectory.

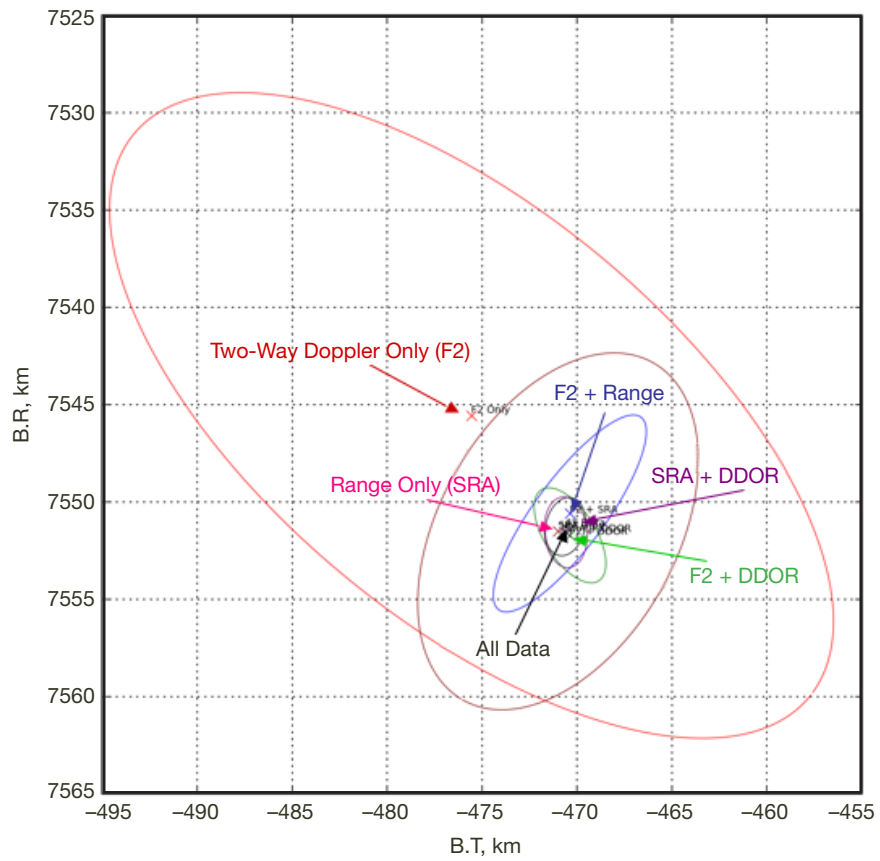


Figure 12. MRO target plane error ellipses just before encounter.

since the errors in the deboost itself then corrupt and dominate the postinsertion solutions. But the predictions are conservative and the 0.4 km uncertainty at the Earth–Mars distance is less than 2 nrad Earth relative. Since these are from formal uncertainty studies and the Mars ephemeris is carried itself at 2 nrad, we believe that the actual estimate was accurate to this level, probably better. This performance is now routinely achieved or exceeded.

The current performance and operational reliability of the Δ DOR system has been achieved via a lengthy evolution process since its seminal beginnings in the late 1970s. We turn now to a brief recap of this history in the following sections.

VI. A Recap of the Development of Δ DOR, Its Performance Validation, and Interactions With the Flight Projects

A. Voyager and Viking: 1979–1989

When first proposed, it was planned that the first implementation for validating the Δ DOR technique would necessarily need to wait until a space-qualified DOR tone generator could be developed and a flight project could be convinced to integrate the tone generator into the RF assembly aboard the spacecraft. But D. Lee Brunn¹⁰ pointed out that the subcarrier of the Voyager spacecraft’s telemetry subsystem and its harmonics could be used as a surrogate tone generator. As this subcarrier was but 360 kHz, it could not pretend to offer the high-precision measurements enabled by a dedicated tone generator, but by employing the harmonics — out to the 9th harmonic of this tone, giving Δ DOR a 6.5-MHz total spanned bandwidth — experiments proving feasibility were quite possible. Voyager was an excellent opportunity, since the differenced two-way range was already planned as an operational capability for the Saturn encounters, as has already been outlined. The opportunity to prove the feasibility of Δ DOR (albeit at the lower bandwidth afforded) and at the same time compare it with its coherent companion in an operational setting was then planned to take place during the two encounters with Saturn.¹¹

Measurements began in 1979. At this time, the DSN stations were equipped with Mk II VLBI systems [27]. All use of the Mk II system was considered to be a “research and development” activity and not operational support. Data from two time-multiplexed frequency channels, each with a bandwidth of 2 MHz, were recorded on magnetic tape. Telemetry subcarrier harmonics ranging from the ± 5 th to ± 9 th were observed. It was believed that accuracy as good as 100 nrad (approximately 80 cm delay error) might be possible. An error budget published in [28] is reproduced in Figure 13.

Signals were detected in the early measurements, but the time delay observables did not appear to be correct. David S. Brown¹² of JPL is credited with the realization that instrumental phase shifts on the baseband spacecraft and quasar signals were not canceling, due to the use of both upper and lower sideband channels in the Mk II VLBI system. This was the last

¹⁰ D. Lee Brunn, personal communication, Jet Propulsion Laboratory, Pasadena, California, circa 1977.

¹¹ Coherent round-trip range measurements were alternately made at two stations separated in time by the round-trip light time.

¹² David S. Brown, personal communication, Jet Propulsion Laboratory, Pasadena, California, circa 1977.

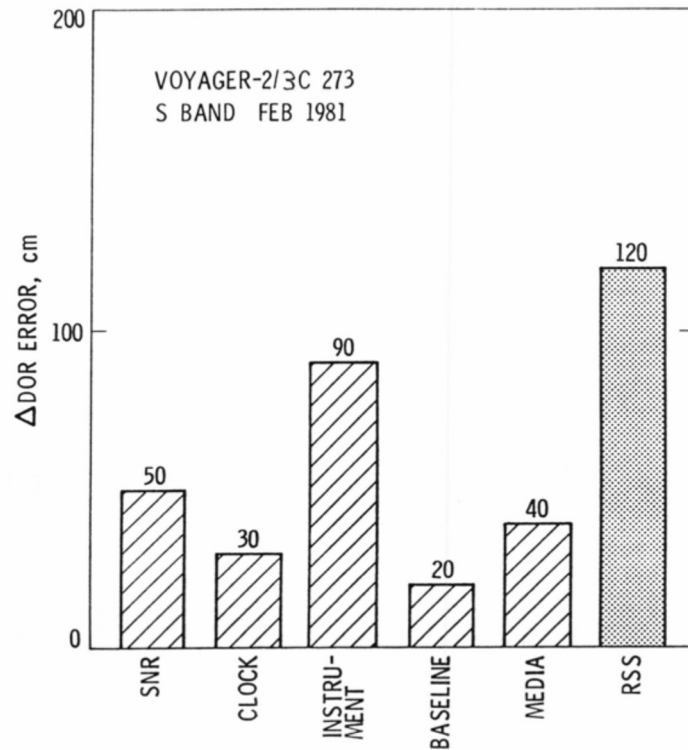


Figure 13. Error budget for Voyager S-band Δ DOR measurements in 1981.

piece of the puzzle necessary to perform Δ DOR. The Mk II frequency downconversion system was modified to use two channels of the same sideband, each centered on the received frequency of a spacecraft tone. Subsequently, data were acquired from both Voyager spacecraft beginning in January 1980 with angular position accuracies approaching 100 nrad, allowing Δ DOR to contribute to the successful Voyager flybys of Saturn as reported by Brown [29] and Taylor [30].

Since the Δ DOR and differenced range results were comparable and because Δ DOR was seen as the wave of the future, all future developments were centered on that and differenced range receded to the background.

Coincident with this, Δ DOR measurements were attempted with the Viking Lander 1, with the simultaneous goals of demonstrating the Δ DOR technique and tying Mars to the radio reference frame [31]. Since the lander position on the surface was known, this would be an ideal frame tie. Because the spacecraft telemetry spectrum did not span enough bandwidth, range tones were transmitted from a ground station, and transponded at the spacecraft, to provide the necessary wide-bandwidth signals for Δ DOR. Unfortunately, only a few measurements could be attempted and time ran out before the technique was made to work with Viking.

The long tour of Voyager 2 through the outer solar system provided the opportunity to develop the Δ DOR technique. A new VLBI system was being implemented in the DSN to provide operational support for measurements of interstation clock synchronization, UT,

PM, and Δ DOR. The implementation was done in phases. In the first phase, completed in January 1981, the Mk II analog baseband signals were sent to an open-loop recorder, used for radio science, known as the occultation data assembly (ODA). The ODA digitized, filtered the channels to a bandwidth of 250 kHz, and recorded the data on a computer tape [32]. Recorded data could be transmitted within hours from the stations to a computer disk at JPL, over links that had been established for communications. Data were correlated first in software on a mainframe computer on the Caltech campus and, by mid-1981, on a dedicated minicomputer at JPL that interfaced with a custom digital signal processor board. Having the data on a random-access disk, instead of a serial-access tape, greatly facilitated the extraction of spacecraft tone phase. Delta-DOR observables could now be delivered to a navigation team within 24 hr whereas previously it had taken weeks to ship magnetic tapes from the DSN stations and process the data on a hardware correlator.

Validation of data correctness was a goal just as important as meeting an accuracy requirement. Side-by-side comparisons of data output were made as new system implementations were completed. Recording systems, correlators, and data processing software were checked against each other. Absolute accuracy was more difficult to assess, although basic consistency was established by showing that spacecraft trajectory solutions with and without Δ DOR agreed within statistical uncertainties.

After the successful Saturn encounters, and with Δ DOR on its way to becoming an operational DSN capability, the Voyager project dropped its requirement for differenced range and used Δ DOR for its Uranus encounter in 1986 and its Neptune encounter in 1989. Final targeting for these encounters relied on the spacecraft camera to image the planet's moons and develop direct knowledge of spacecraft position relative to the planet. Delta-DOR was employed during cruise to maintain the radiometric solution and approach trajectory within an acceptable level of uncertainty so only small trajectory correction maneuvers would be necessary once camera images located the spacecraft position relative to the planet.

A demonstration of improved accuracy for Δ DOR measurements was begun in 1982 to help validate the technique for planned use by the Galileo mission to Jupiter. Observation frequencies were switched from S-band to X-band. While supporting the first X-band test at Goldstone, Lyle Skjerve noticed higher-order even harmonics in the downlink signal spectrum. Though only odd harmonics were expected in the spectrum of the square-wave telemetry subcarrier, the phenomenon was quickly explained by Claude Hildebrand and Thomas Yunck. The stronger X-band signal allowed detection of higher-order telemetry subcarrier harmonics spanning 14 MHz, and further, reduced the effects of charged particles. A greater number of passes was scheduled to investigate internal data consistency and measurement errors. Internal consistency at the 25-nrad level was obtained [28] but biases and drifts over a few-month period were larger by an order of magnitude. Eventually it was understood that these offsets were due to inconsistencies in the tie between the radio catalog and the outer planet ephemeris that, at the time, was based solely on optical data.

The final phase of the narrow-channel bandwidth (NCB) VLBI system was completed in 1985 [33]. The analog portion of the Mk II VLBI system was replaced with hybrid analog and digital components. The name for this system derived from its modest sampling rate

as compared to systems built for astronomy research. The 0.5 megabits/s sample rate allowed for near-real-time data transfer, necessary for navigation support, but also limited system sensitivity. A key design feature was the time multiplexing of signals at intermediate frequency, enabling all baseband (video) signals to pass through the same analog-to-digital converter and digital low-pass filter. This was necessary to reduce instrumental phase differences between spacecraft and quasar signals and to allow group delays over a bandwidth of 40 MHz to meet the 50-nrad accuracy requirement.

Almost all measurements during this time were made using a standard sequence of a 9-min spacecraft observation followed by a 9-min quasar observation. Experimental variations were avoided so as to minimize the impact on the project. The Δ DOR development effort and the Voyager project benefited from each other during this decade, but it should be acknowledged that Δ DOR was not a critical data type for Voyager or any other project during this time period. As a result, Δ DOR was vulnerable to budgetary review and reductions in the DSN budget.

B. Magellan, Galileo, and Mars Observer: 1989–1997

Though the Galileo launch was delayed, and there would be no close flyby of Mars, Δ DOR had become a requirement for the Magellan cruise phase to Venus, the Galileo flybys of Earth followed by its cruise to Jupiter, and the Mars Observer cruise phase. Use of Δ DOR allowed reductions in the amount of tracking time needed to collect coherent Doppler for navigation, provided an independent cross-check on trajectory solutions, and maintained accurate targeting so as to reduce fuel usage for corrective maneuvers. An important lesson learned from the Voyager demonstration was to record more than the minimum amount of data necessary to generate a time delay observable. At least three observations, either in sequence spacecraft–quasar–spacecraft or quasar–spacecraft–quasar, were recorded to estimate station clock offsets and drifts and to help identify any temporal variations such as a jump in the station clock. Also, at least three frequency channels were recorded in order to identify any dispersive instrumental error such as multipath at one frequency. These additional data allowed for internal validation of the measurement prior to delivery to the navigation team.

Encouraging results from the Voyager demonstration, good instrumental design of the new NCB VLBI system, and ongoing improvements in related calibration systems led to expectations that performance would be better than the original 50-nrad accuracy requirement.

The Magellan mission was designed to make high-resolution radar maps of the Venus surface. Though the transponder did not have DOR tones, the high-rate telemetry system needed to send the radar data back to Earth had sidebands spanning 30 MHz at X-band, providing a good signal for Δ DOR observations. But most of the cruise passes were scheduled on DSN 34-m antennas as opposed to early Voyager Δ DOR passes that mostly used 70-m antennas. While the wide signal bandwidth drove some error sources down, the smaller ground apertures forced selection of stronger radio sources at greater angular separations from the spacecraft. Magellan was observed during cruise from July 1989 to August 1990 with typical data accuracy of 30 nrad. The targeting for orbit insertion was so accurate

that no orbit trim maneuvers were needed for the scientific mission to begin [34]. Magellan was observed in orbit at Venus from September 1990 to August 1994, with a typical data accuracy of 20 nrad, to establish a better radio–planetary frame tie.

The Galileo mission began with several flybys of inner planets for gravitational assists, and the spacecraft visited two asteroids before heading to Jupiter. The spacecraft communicated through its low-gain antenna at S-band while in the inner solar system, providing a bandwidth of 7.65 MHz for Δ DOR. Measurements were acquired from January 1990 to December 1993 with an accuracy of 50 nrad. The restricted bandwidth and the larger effects of charged particles at the S-band frequency prevented higher accuracy. The mission was replanned during flight, when the spacecraft high-gain antenna failed to deploy, and the requirement for Δ DOR on approach to Jupiter was dropped. But Δ DOR was obtained during the orbital phase from July 1996 to September 1997 for the purpose of tying the position of Jupiter to the inner planets [35].

Mars Observer was the first spacecraft to transmit DOR tones with the full spanned bandwidth of 38.25 MHz at X-band. By this time, operational procedures had been streamlined and Δ DOR was becoming a routine DSN capability. The spacecraft was observed throughout cruise from October 1992 to August 1993, with a data accuracy of 23 nrad. However, only three days prior to the planned arrival at Mars, communication with the spacecraft was lost. By all accounts, Mars Observer had been on course for an accurate insertion into orbit about Mars [36].

While, as for Voyager, Δ DOR was beneficial for these missions, it could not be said that it was essential for mission success. Even though Δ DOR had performed well as a navigation tool during this decade, missions planned for the late 1990s did not identify a critical need for this capability and dropped requirements for Δ DOR as part of cost-cutting moves

VII. Mars Program: 2001–2012

Mars Climate Orbiter, while originally planned to employ Δ DOR, had this requirement dropped for cost-cutting reasons. The mission relied on two-way range and Doppler, which under normal circumstances would have sufficed. Unfortunately, there was an error in establishing the units for impulses from the small thrusters that were used to desaturate the momentum wheels, in order to control spacecraft attitude. This misunderstanding led to mismodeling of these forces and ultimately to a navigation error at the time of MOI so large as to cause impact with the planet. The NASA review board identified this error as the root cause of the mishap detailed in their Phase I report [37].

This was the root cause of the problem, but a more proximate cause was a failure to identify this problem early enough to correct it. And it was soon recognized by both the project and the DSN alike that, had Δ DOR been available, the mission would most certainly have been saved.

Following the failures of two Mars missions in 1999, NASA reinvigorated its Mars program with renewed emphasis on robustness and reliability. Delta-DOR and onboard optical imag-

ing were alternately considered as methods to ensure navigation success and Δ DOR was quickly adopted. Collateral developments made it possible to put together a new system for Δ DOR observations, much improved over previous implementations, in time for the launch of Mars Odyssey in April 2001. The procedural and component designs that made this possible are discussed in the next section of this article as is the role that these implementations ultimately had on the projects' conduct of the navigation.

Delta-DOR served its purpose for the Odyssey spacecraft by providing a cross-check on navigation solutions and ensuring successful targeting for Mars orbit insertion. Excellent results were obtained for cruise navigation [38] with the new Δ DOR system delivering accurate data within 12 to 24 hr, with high reliability. This inflight success drew the attention of the Mars Exploration Rover (MER) development team. The MER project evaluated the possibility of using Δ DOR to reduce the size of its landing error ellipse. Significantly, new science opportunities emerged when the decision was made to use Δ DOR in this way, as improved targeting enabled more landing site options [39]. Delta-DOR was now serving its intended purpose as a critical part of mission operations. The Δ DOR system again performed well and navigation delivery accuracy was excellent for both rovers in 2003–2004 [40].

By default, Δ DOR is now considered a key data type for any mission needing to navigate precisely through the solar system. Delta-DOR was used by Mars Reconnaissance Orbiter (MRO) in 2005 for insertion into orbit, as described in [41] and Section V of this report, and by Phoenix in 2007–2008 to land on the Martian surface [42], both with excellent results. Mars Science Laboratory (MSL), planned for launch in 2011, requires Δ DOR to support targeting accuracy similar to what was needed for Phoenix, but also requires a late knowledge update to initiate onboard guidance systems for controlled descent through the atmosphere.¹³ The DSN Δ DOR service now meets expectations in terms of relevance, accuracy, reliability, and ease of use.

VIII. Operational and Performance Considerations

Delta-DOR began as an experiment conducted outside the normal scope of DSN operations. It had been necessary to adapt and make use of research equipment and techniques due to long lead times for spacecraft and DSN implementations. Since Δ DOR passes were infrequent compared to the normal tracking passes performed by the DSN, the manual steps necessary for data acquisition were problematic. Even worse, missions had an awkward time placing the sequence steps for a Δ DOR observation into their timelines. By the 1990s, Δ DOR had become unpopular due to its perceived lack of reliability and its difficult interfaces with the missions. Table 1 shows the number of scheduled observations and the success rate for several missions over the past three decades. The data accuracy, presented as the rms of residuals, is also shown for the Mars missions. This was calculated using the final reconstructed cruise trajectory for each mission.

Early on, the Δ DOR technique could be made to work well, but failures still occurred for various reasons. The success rate achieved in the 1980s and 1990s did not match the 99 per-

¹³ The DSN radiometric tracking system performed as expected for Mars Science Laboratory, delivering the spacecraft to the top of the Martian atmosphere with accuracy of 1 nrad.

Table 1. Number of scheduled Δ DOR observations, success rate, and data accuracy over three decades.

Spacecraft	VLBI System	Period	Number of Scheduled Observations	Success Rate	Residual RMS, nrad
Voyager	Mk II + ODA	1981–1984	144	67%	N/A
Vega	NCB	1985–1986	62	97%	N/A
Voyager	NCB	1986–1987	90	62%	N/A
Phobos	NCB	1988	21	81%	N/A
Magellan (cruise)	NCB	1989–1990	56	86%	N/A
Galileo	NCB	1990–1992	48	88%	N/A
Mars Observer	NCB	1992–1993	66	86%	22.5
Mars Odyssey	RSR	2001	48	98%	4.50
MER	VSR	2003–2004	131	98%	1.61
MRO	VSR	2005–2006	65	98%	1.18
Phoenix	WVSR	2007–2008	105	100%	1.09

cent success rate expected of conventional DSN tracking activities. Most failures could be broadly grouped into two categories: (i) error in manual procedure, and (ii) equipment failure. When there was an opportunity to reimplement the Δ DOR system to support the Mars program beginning in 2000, new emphasis was placed on operational considerations. Modernization tasks in the DSN in the 1990s plus development of a new system for telemetry arraying¹⁴ made it possible to fully integrate Δ DOR data acquisition into DSN operations. Further, the flight projects were coached to develop scheduling and sequencing tools to support Δ DOR. A flexible interface was developed to select quasars to be observed as well as the number and duration of alternate spacecraft and quasar observations. At the preliminary design review for Δ DOR development for Mars Odyssey in 2000, it was stated that system reliability should be no worse than that expected for two DSN stations to perform conventional tracking activities at the same time, that is, 0.99². A success rate close to this value has been obtained for over 1000 observations spread across 16 missions since 2000.

A. International Acceptance

If Δ DOR measurements have been important for NASA missions, what about for missions of other space agencies? Both the European Space Agency (ESA) and the Japan Aerospace Exploration Agency (JAXA) have negotiated agreements with NASA for the DSN to provide Δ DOR measurements to support their missions. Support for ESA has included the Rosetta, Mars Express, and Venus Express missions. Support for JAXA has included the Nozomi, Hayabusa, and Akatsuki missions. More recently, ESA has developed its own Δ DOR capability for use in the ESA deep-space tracking network [43]. Similarly, JAXA is developing Δ DOR capability [44]. Both agencies plan on incorporating DOR tones in spacecraft transponders for future missions.

The importance of Δ DOR for high-precision navigation in deep space, and the benefit of combining tracking assets of multiple agencies to provide cross-support, has been gener-

¹⁴ The telemetry arraying system was based on a design for a VLBI upgrade that had been proposed for the DSN but not funded in 1992. Array system components provided all the functionality needed for VLBI.

ally recognized by the world community. Combining multinational assets to support Δ DOR follows the same rationale as the combining of assets some three decades earlier to support astrometric VLBI. The Interagency Operations Advisory Group (IOAG)¹⁵ recommended that the Δ DOR technique be standardized to facilitate interagency cross-support. To further this goal, the Consultative Committee for Space Data Systems (CCSDS) formed a working group to develop standards for Δ DOR and to validate procedures for cross-support. Standards, as they are published, are available on the CCSDS website.¹⁶

B. Error Budget Development and System Innovations

Estimating the uncertainty in a Δ DOR measurement has always been an important aspect of the technique, both as an aid to system development and to allow valid assessment of accuracy for navigation targeting. The earliest writings on Δ DOR [45] contained a breakout of the components that contribute to measurement error, including assumptions about geometry, recording sequence, calibration, and a calculation of error magnitude. A total error was calculated as the root-sum-square (rss) of the components. This breakout became known as the Δ DOR error budget. A new error budget was developed for each mission, based on spacecraft characteristics, trajectory geometry, and current DSN capabilities. While conditions would vary from one pass to another, the error budget was meant to represent the performance that the mission could count on. The larger error sources were studied by DSN technology development tasks and recommendations were made for improving system performance. Since most components of the error budget affected range and Doppler as well as Δ DOR, system upgrades would provide synergistic improvements to all radiometric tracking techniques. But implementation in the DSN is driven by new mission requirements, available technology, and trade-offs between cost and performance, so program-level justification was required for system upgrades.

The error budget published for Voyager in 1980 [29] shows an rss error of 135 nrad. The dominant component is dispersive instrumental phase due to the restricted bandwidth (3–6 MHz) of the spacecraft signal. Performance improvement had to wait for spacecraft with wider bandwidth signals. To investigate the error budget for the Galileo mission, experiments were planned to observe pairs of natural radio sources using a 38-MHz spanned bandwidth [46]. The Δ VLBI time delay error was investigated as a function of source separations, source elevations, source strengths, solar plasma, and ionosphere. It was found that the 50-nrad requirement could be met for source separations as large as 25 deg.

When spacecraft signals with wider bandwidths were observed starting in 1989, the errors due to dispersive instrumental phase and thermal noise came down, and the rss error fell to the 20–30 nrad level. But now all error components were roughly of the same magnitude, implying that significant development would be needed to further improve system performance.

¹⁵ <https://www.ioag.org/default.aspx>

¹⁶ <http://public.ccsds.org/default.aspx>

Data from all missions have been analyzed to verify and improve upon Δ DOR error budget estimates. It is especially instructive to examine measurement residuals to a reconstructed trajectory for which navigators can establish an independent estimate of trajectory accuracy that can serve as a “truth model.” The error budgets presented in this article have all been verified by analyses of this type. It should be noted that the residual rms obtained during cruise may slightly underestimate the true measurement error, since the spacecraft trajectory has been adjusted to fit the data. A more rigorous test of absolute accuracy is provided by analysis of data obtained from Mars orbit, as explained in Section IX.

C. System Improvements: 1993–2000

The last operational use of Δ DOR to support spacecraft navigation, prior to Mars Odyssey in 2001, was for the Mars Observer mission in 1992–1993. During this hiatus, a number of system improvements occurred that would benefit new users. The most important of these are discussed below.

DSN Operations

Three upgrades in the DSN led to improved overall reliability and operability. First, anticipating the challenges of spacecraft communications at Ka-band, antenna-pointing models were improved. Blind pointing, that is, pointing to a predicted angular coordinate without real-time feedback, became more reliable. Second, new microwave controllers allowed setting and monitoring of the downlink signal polarization from the operator’s console. Third, distribution of intermediate-frequency signals within the station was automated. Though these upgrades were not driven by Δ DOR, they ensured the correct downlink signal would be routed to the VLBI system.

VLBI System

A new VLBI system for downconverting and recording signals was developed to replace the NCB system. The new system was based on the full-spectrum recorder [47] that had been developed to support Galileo telemetry arraying. The first version of the new system to support the wide bandwidth recordings needed for quasar observations was the radio science receiver (RSR). As the name suggests, this system was primarily developed to support radio science applications, but was initially shared between radio science and VLBI. In 2003, another version of this system, known as the VLBI science receiver (VSR), was implemented to provide dedicated support for VLBI applications. The system front-end bandwidth was increased in 2005 and named wideband VSR (WVSR) [48]. The RSR, VSR, and WVSR had several major advantages over the NCB system. The control interface was robust and allowed real-time monitoring of signal acquisition. The digital finite-impulse response filters used for narrowing the input bandwidth had purely linear phase response, eliminating a major source of instrumental error. The system was capable of recording rates as high as 80 megabits/s, in contrast to the 0.5 megabits/s capacity of the NCB system. This higher record rate, coupled with increased communications bandwidth to provide playback of the greater data volume, allowed a corresponding increase in precision. In addition, the data-correlation algorithm was improved to generate time-delay observables with sub-cm model accuracy to realize the full precision available from the data. A functional description of the current recording system can be found in [49].

GPS Calibration System

The DSN's GPS calibration system had become operational for providing parameters used to model signal delay through the troposphere and ionosphere, and to model the orientation of the Earth in inertial space. These calibrations provided a significant improvement in accuracy, with reduced latency, compared to the calibrations available before GPS data were used.

Model Consistency

The consistency of models used for development of the radio reference frame and for spacecraft navigation should also be mentioned. Model inconsistencies could prevent the full accuracy of Δ DOR measurements from being utilized in spacecraft navigation. In the early 1990s, a working group was formed at JPL to examine reference frame issues. As a result, models were added to the JPL navigation software to allow accurate transformations between the recommended terrestrial and celestial systems. The International Celestial Reference Frame (ICRF) [24] defined by the positions of radio sources was adopted as the fundamental celestial frame.

D. System Improvements: 2001–2003

The actual performance of the Δ DOR measurement system improved further by 2003 due to several other factors.

Improved Station Locations

The station locations used for the first look at data from Mars orbit, and to support the Odyssey mission, were based on a 1993 solution. Continental drift was not accurately modeled over the following 10 years, and the newer DSN 34-m stations were not accurately surveyed. Modeling improved when a new joint solution for DSN station locations was completed in 2003, and referenced to epoch 2003.

Improved Quasar Catalog

The first look at data from Mars orbit, and the Odyssey cruise measurements, used the published ICRF Extension 1 (ICRF-Ext-1) catalog [50]. This catalog, while defining a reference system, was not optimal for supporting differential astrometry using specific sources. A new solution was generated at JPL using more long-baseline DSN data. This solution added a substantial number of new measurements and reduced systematic errors, especially for southern hemisphere sources, relative to ICRF-Ext-1. For the first time, good positions were obtained for certain sources that had relatively few observations in the data set used for ICRF-Ext-1.

Global Ionosphere Maps (GIM)

The ionosphere calibrations used for the first look at data from Mars orbit and for Odyssey cruise supports were based on single-shell, single-GPS receiver data sets. A substantial improvement occurred when a new calibration system that incorporated multiple receivers near each site and multiple shell models was implemented in 2003.

Observation Technique

A higher sampling rate was used for quasar recording that allowed more precise time delays or use of weaker sources that were closer in an angular sense to the spacecraft trajectory. Multiple quasars were observed, with one on either side of the spacecraft when possible, to provide improved cancellation of spatial errors. Further, observations were scheduled to avoid the lowest elevation angles.

E. Evolution of System Performance and Future Prospects

The performance of the Δ DOR system over its three decades of existence is shown in Figure 14. Missions that provided drivers for system improvements are used to illustrate performance over different eras and the key system upgrades and innovations are identified. Delta-DOR was also used to support numerous other missions during the times shown with similar levels of performance. The current Δ DOR error budget is shown in Figure 15 [51]. Comparing with Figure 13 shows technology improvements in all facets of the technique. Key assumptions used to estimate the terms in the current error budget are shown in Table 2.

Note that a measurement angular accuracy of 1 nrad, at the typical Earth–Mars distance of 1 AU for encounter geometry, corresponds to 150 m in POS position. This accuracy meets or exceeds current navigation needs for targeting a descent module to the top of the Martian atmosphere.

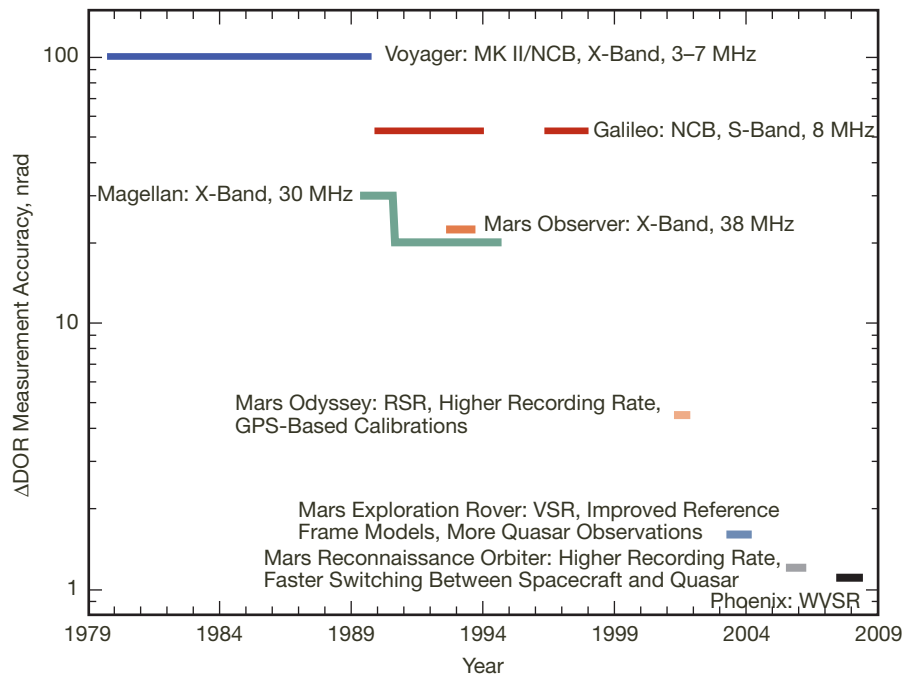


Figure 14. Evolution of Δ DOR system performance.

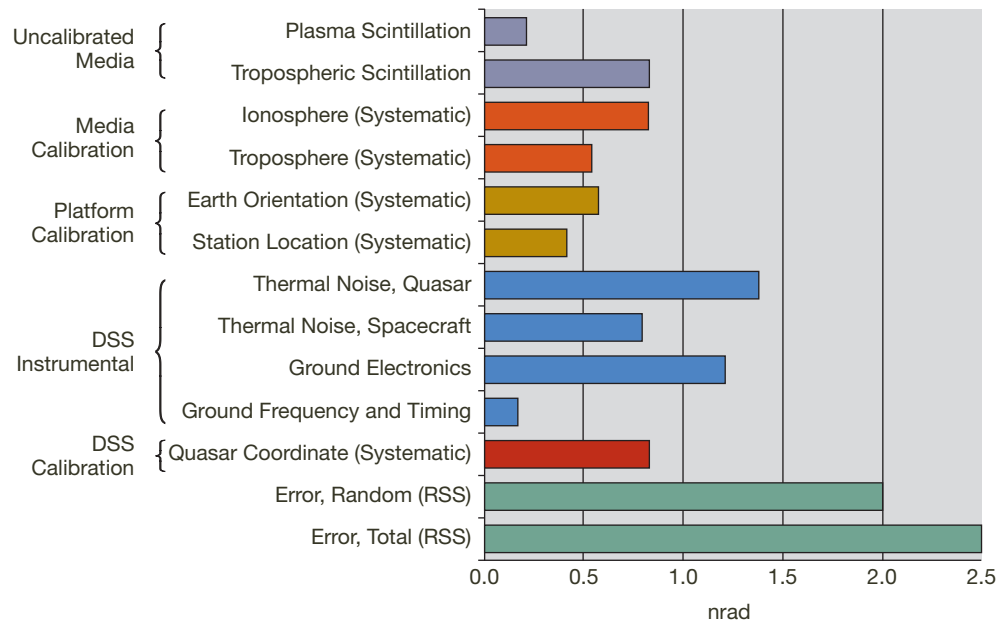


Figure 15. Δ DOR error budget for 2009.

Table 2. Key Δ DOR error budget assumptions.

Term	Assumption
Spacecraft transmitter	± 19 MHz DOR tones at X-band
Media path delays	Surface meteorological data and GPS satellite observations from multiple receivers near tracking stations are used to develop calibrations [52,53]
Platform parameters	VLBI data and GPS satellite observations from a global network are used to develop calibrations [54]
Spacecraft–quasar angular separation	6 deg separation between spacecraft and virtual quasar at arc midpoint between two actual quasars
Quasar flux	0.4 Jy
Receiver bandpass phase ripple	0.2 deg for 4-MHz channel bandwidth

Performance for X-band measurements is now approaching a fundamental limit set by the available spanned bandwidth. But some ideas are being investigated to work around this seeming limitation. To begin, the WVSr in the DSN is now being upgraded to enable data recording at a rate as high as 256 megabits/s. This makes it feasible to record across a wider spanned bandwidth and with enough sensitivity to detect the weaker radio sources that nearly fill the sky. The JPL radio source catalog has now expanded to over 3600 sources [55]. Approximately 700 sources have well-known coordinates. It is generally possible today to select well-known sources with adequate flux to provide a virtual quasar within 6 deg angular separation from most any point along the ecliptic.¹⁷ Extension of the catalog is expected to continue, so that reference sources would be available within 1–2 deg of most any point along the ecliptic [56]. Figure 10 shows the current status of densifying the catalog along the planned MSL trajectory. Selecting a reference source angularly close to the spacecraft reduces platform and media effects, while recording across a wider bandwidth improves precision. However, it is not straightforward to apply these improvements.

Recall from Section VI that the earliest attempts at Δ DOR measurements suffered from noncanceling instrumental effects between the spacecraft and quasar signals. With spacecraft transmissions still limited to about 40 MHz spanned bandwidth, care must be taken to avoid an instrumental bias introduced by observing quasars across a wider bandwidth. Three separate approaches to work around this potential instrumental bias are being considered. In the first approach, a very strong quasar is observed both at the spacecraft downlink frequencies and at much wider spaced frequencies near the receiver bandpass edge. Data from this quasar are used to develop a calibration for the instrumental offset between the different observing frequencies [57]. A (typically much weaker) reference source, angularly close to the spacecraft, is selected for Δ DOR, its delay is precisely measured using the widest bandwidth, and then this delay is calibrated to instrumentally align with the delay at the spacecraft downlink frequencies.

In the second approach, the measurement is made not over some 40-MHz-spanned bandwidth, but with the X-band RF carrier wave itself. As explained in Section III, it is not possible in general to resolve the cycle ambiguity at RF, except in this case only a narrow-angle differential measurement is being attempted. The geometric data strength obtained from observing over some fraction of the full DSN baseline view period might make ambiguity resolution possible [58]. Alternatively, the first approach described just above might improve group delay accuracy enough to step wise resolve the cycle ambiguity at RF.

Both the first and second approach determine spacecraft position relative to a quasar. Today, global quasar astrometry is at about the 0.5-nrad level. This is still a limit to the absolute accuracy that can be obtained from Δ DOR. The third approach to improve accuracy works around this limitation also. For many cases where very high Earth-based navigation accuracy is needed, the target is a well-known object such as Mars and already has orbiting or landed spacecraft that transmit to the DSN. One of these spacecraft can be used as the reference source instead of a quasar. For Mars, the arriving spacecraft is typically within 1 deg of Mars for the final 30 days of approach. But a strategy is again needed

¹⁷ The location at right ascension 18 hr, declination –23 deg, near the intersection of the ecliptic and galactic planes, is particularly challenging, and performance drops off in this vicinity.

for RF cycle ambiguity resolution [59]. The strategy would likely be a combination of the first and second approaches described above. If the ambiguity can be resolved, then angular accuracy as good as 0.1 nrad would be expected for the position of the approaching spacecraft relative to its intended target. Navigators have expressed interest in such a capability, primarily to obtain quicker knowledge of encounter coordinates following the final targeting maneuver [60].

More generally, a further significant advance in the Δ DOR technique is expected when spacecraft downlinks transition from X-band to Ka-band. This transition is being driven by the need for more telecommunications bandwidth, and also by crowding of the spectrum at X-band. There are three immediate advantages: a wider spanned bandwidth is allowed for DOR tones, charged-particle effects are reduced, and quasar cores are more compact. Work has already begun on development of a quasar catalog at Ka-band [61]. With effort, the Δ DOR error budget can be revisited and system improvements can be planned to further reduce the dominant error sources.

IX. Frame Tie

The first significant advance to tie the radio frame to the planetary frame, since the 100-nrad tie using VLBI measurements of planetary orbiters in the early 1980s, came in 1993 through joint analysis of lunar laser ranging data and VLBI data [62]. Though indirect, this method provided knowledge of the positions of the inner planets in the radio frame with 15-nrad accuracy. Delta-DOR measurements of Magellan at Venus in 1990–1994 confirmed this tie and improved the accuracy to 5 nrad. However, even better accuracy was desired to support missions sending a lander direct from Earth to the surface of Mars.

The Mars missions themselves provide the infrastructure to improve the frame tie. Further, Δ DOR measurements of spacecraft at Mars provide the best means to establish the absolute accuracy of the Δ DOR technique. Nothing has been left to chance. A few Δ DOR measurements of Mars Global Surveyor (MGS) were obtained in early 2001 using the newly developed RSR-based Δ DOR system. Since the MGS orbit was known relative to the Mars center to about 20 m, the Δ DOR residual (that is, the observed value minus the best model value) provided a direct measure of the Mars position error and/or the Δ DOR measurement error. The residuals from both DSN baselines were at the 5-nrad level, providing confidence both in the planetary ephemeris and in the new Δ DOR system for support of Odyssey.

After Odyssey orbit insertion, enough Δ DOR measurements were obtained from MGS and Odyssey to fully determine the orientation of the planetary ephemeris in the radio frame with 2-nrad accuracy. The fit of the data over a synodic period of Mars ruled out any bias in the Δ DOR system and verified the absolute accuracy of the data. This provided the verification necessary for the planned use of Δ DOR to support the MER landings. Since MRO orbit insertion, Δ DOR data are being acquired at the rate of one per month from Odyssey and MRO to improve accuracy of the Mars ephemeris to better than the 1-nrad level for MSL.

Figure 16 shows the residuals, with error bars, of all Mars orbiter Δ DOR observations.¹⁸ The two plots are for the two DSN baselines. The planetary ephemeris has been rotated to align with the radio reference frame, removing what would have been a 5-nrad systematic offset. However, the shape of the Mars orbit is strongly determined by spacecraft ranging data, and the Mars ephemeris cannot be empirically adjusted to perfectly fit the Δ DOR data. Hence, these Δ DOR residuals provide a measure of the total error in the technique. Note how measurement accuracy has improved from 2001 to 2011, consistent with Figure 14. These data are the best laboratory for the study and improvement of the Δ DOR technique. Some measurements, including some with small error bars, and including some systematic clumps of measurements, appear to be offset by up to 2 sigma. Partial understanding of these offsets has been found. Unexpected errors of this magnitude may be caused by ionospheric delay mismodeling for poor observation geometries or by radio source structure effects on the long DSN baselines. Lessons learned from these data are incorporated into future observation plans. There is still more to learn, but it is clear that data accuracy can routinely be

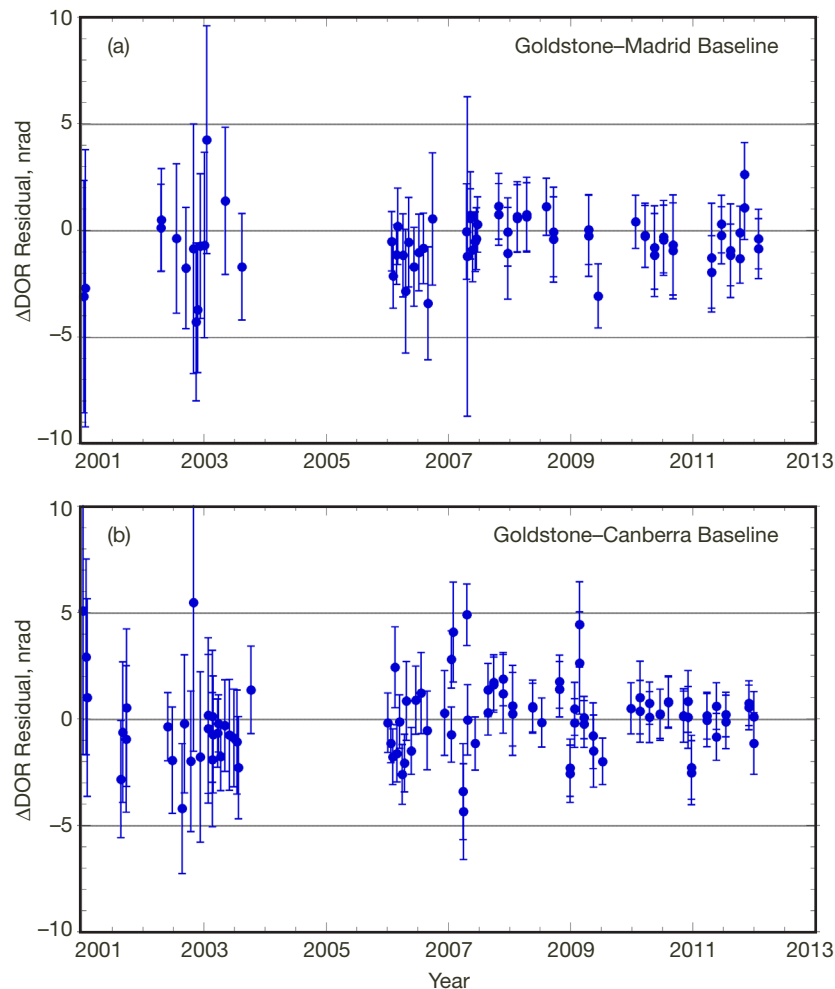


Figure 16. Residuals of Δ DOR observations of Mars-orbiting spacecraft.

¹⁸ W. M. Folkner and J. S. Border, "Linking the Planetary Ephemeris to the International Celestial Reference Frame," to appear in *Highlights of Astronomy*, vol. 16, T. Montmerle, ed., XXVIIIth IAU General Assembly, August 20–31, 2012, Beijing, China.

obtained at the level of 2 nrad or better. Also, it is important to note that the ephemeris of Mars is perturbed by asteroids, so ongoing Δ DOR measurements are needed to maintain Mars ephemeris accuracy at the nanoradian level.

X. Summary

From the earliest missions to the inner planets, two-way range and Doppler were the work-horse data used by the navigation system, and these were developed and refined to their maximum inherent accuracies. As the inner planets were visited, the planetary ephemerides were also improved by these encounters through the opportunities they afforded to tie in the ephemerides to that same range-Doppler tracking system. During the development of the navigation system for Voyager, it was recognized that the one weakness in the refined range-Doppler system was its poor performance at zero declination. Accordingly, the explicit differencing of two-way ranging data using intercontinental baselines was brought to the forefront to cure that weakness. And to improve the monitoring of PM, UT variations, and station-clock synchronization, the VLBI system was introduced as an allied, but independent, system. Slowly the understanding and appreciation of the benefits of tying these systems together developed during Voyager operations and Viking Lander monitoring. Abandoning the explicit differencing of ranging data and instead moving to what is now called the Δ DOR system, by broadcasting suitable waveforms directly from the spacecraft, paved the way for the merging of these systems. This enabled the achievement of inherent accuracies fully two orders of magnitude better than was possible when the systems were operating individually. The fundamental coordinate system is now referred to the nearly invariant quasar-based frame and spacecraft are navigated via measurements that couple to and precisely relate themselves to this frame. These developments, as this article has shown, came neither easily nor quickly, but the current systems now routinely deliver reliable operation at the 98 percent goal and with accuracies approaching 1 nrad.

References

- [1] T. E. Bell, "Quest for the Astronomical Unit," *The Bent of Tau Beta Pi*, Summer 2004.
<http://www.tbp.org/pubs/Features/Su04Bell.pdf>
- [2] W. K. Victor, R. Stevens, and S. W. Golomb, eds., *Radar Exploration of Venus*, Technical Report 32-132, Jet Propulsion Laboratory, Pasadena, California, August 1961.
- [3] W. G. Melbourne, J. D. Mulholland, W. L. Sjogren, and F. M. Sturms, Jr., *Constants and Related Information for Astrodynamical Calculations*, 1968, Technical Report 32-1306, Jet Propulsion Laboratory, Pasadena, California, July 15, 1968.
- [4] J. O. Light, "An Investigation of the Orbit Redetermination Process Following the First Midcourse Maneuver," *Space Programs Summary*, vol. IV, no. 37-33, Jet Propulsion Laboratory, Pasadena, California, June 30, 1965.
- [5] T. W. Hamilton and W. G. Melbourne, "Information Content of a Single Pass of Doppler Data from a Distant Spacecraft," *Space Programs Summary*, no. 37-39, vol. III, Jet Propulsion Laboratory, Pasadena, California, May 31, 1966.
http://descanso.jpl.nasa.gov/History/pdf/sps37-39v3_p18-23.pdf

- [6] S. P. Synnott, A. J. Donegan, J. E. Riedel, and J. A. Stuve, "Interplanetary Optical Navigation — Voyager Uranus Encounter," *Astrodynamics Conference*, Williamsburg, Virginia, August 18–20, 1986, *Technical Papers (A86-47901 23-13)*, pp. 192–206, New York, American Institute of Aeronautics and Astronautics, 1986.
- [7] J. H. Lieske, "Galilean Satellites and the Galileo Space Mission," *Celestial Mechanics and Dynamical Astronomy*, vol. 66, no. 1, pp. 13–20, March 1996.
- [8] O. H. von Roos, "Analysis of the DRVID and Dual Frequency Tracking Methods in the Presence of a Time-Varying Interplanetary Plasma," *The Deep Space Network Progress Report*, Technical Report 32-1526, vol. III, March and April 1971, Jet Propulsion Laboratory, Pasadena, California, pp. 71–76, June 15, 1971.
http://ipnpr.jpl.nasa.gov/progress_report2/III/IIIJ.PDF
- [9] C. C. Counselman III, H. F. Hinteregger, and I. I. Shapiro, "Astronomical Applications of Differential Interferometry," *Science*, vol. 178, pp. 607–608, November 1972.
- [10] T. A. Clark, "Building the Geodetic VLBI Network," presentation to Institute of Applied Astronomy of the Russian Academy of Sciences, Saint Petersburg, Russia, February 10, 2005.
<http://ivscc.gsfc.nasa.gov/pub/TOW/tow2005/notebook/Clark.Lec.pdf>
- [11] J. L. Faselow, P. F. MacDoran, J. B. Thomas, J. G. Williams, C. J. Finnie, T. Sato, L. Skjerve, and D. J. Spitzmesser, "The Goldstone Interferometer for Earth Physics," *The Deep Space Network Progress Report*, Technical Report 32-1526, vol. V, July and August 1971, Jet Propulsion Laboratory, Pasadena, California, pp. 45–57, October 15, 1971.
http://ipnpr.jpl.nasa.gov/progress_report2/V/VH.PDF
- [12] P. R. Dachel, S. M. Petty, R. F. Meyer, and R. L. Sydnor, "Hydrogen Maser Frequency Standards for the Deep Space Network," *The Deep Space Network Progress Report*, vol. 42-40, May and June 1977, Jet Propulsion Laboratory, Pasadena, California, pp. 76–83, August 15, 1977.
http://ipnpr.jpl.nasa.gov/progress_report2/42-40/40I.PDF
- [13] J. B. Thomas, "An Analysis of Long Baseline Radio Interferometry," *The Deep Space Network Progress Report*, Technical Report 32-1526, vol. VII, November and December 1971, Jet Propulsion Laboratory, Pasadena, California, pp. 37–50, February 15, 1972.
http://ipnpr.jpl.nasa.gov/progress_report2/VII/VIIIG.PDF
- [14] J. B. Thomas, "An Analysis of Long Baseline Radio Interferometry, Part II," *The Deep Space Network Progress Report*, Technical Report 32-1526, vol. VIII, January and February 1972, Jet Propulsion Laboratory, Pasadena, California, pp. 29–38, April 15, 1972.
http://ipnpr.jpl.nasa.gov/progress_report2/VIII/VIIIG.PDF
- [15] J. B. Thomas, "An Analysis of Long Baseline Radio Interferometry, Part III," *The Deep Space Network Progress Report*, Technical Report 32-1526, vol. XVI, May and June 1973, Jet Propulsion Laboratory, Pasadena, California, pp. 47–64, August 15, 1973.
http://ipnpr.jpl.nasa.gov/progress_report2/XVI/XVIK.PDF

- [16] J. I. Molinder, "A Tutorial Introduction to Very Long Baseline Interferometry (VLBI) Using Bandwidth Synthesis," *The Deep Space Network Progress Report*, vol. 42-46, May and June 1978, Jet Propulsion Laboratory, Pasadena, California, pp. 16–28, August 15, 1978.
http://ipnpr.jpl.nasa.gov/progress_report2/42-46/46C.PDF
- [17] A. E. E. Rogers, "Very Long Baseline Interferometry with Large Effective Bandwidth for Phase-Delay Measurements," *Radio Science*, vol. 5, no. 10, pp. 1239–1247, October 1970.
- [18] M. A. Slade, P. F. MacDoran, and J. B. Thomas, "Very Long Baseline Interferometry (VLBI) Possibilities for Lunar Study," *The Deep Space Network Progress Report*, Technical Report 32-1526, vol. XII, September and October 1972, Jet Propulsion Laboratory, Pasadena, California, pp. 35–39, December 15, 1972.
http://ipnpr.jpl.nasa.gov/progress_report2/XII/XIII.PDF
- [19] M. A. Slade, P. F. MacDoran, I. I. Shapiro, D. J. Spitzmesser, J. Gubbay, A. Legg, D. S. Robertson, and L. Skjerve, "The Mariner 9 Quasar Experiment: Part I," *The Deep Space Network Progress Report*, Technical Report 32-1526, vol. XIX, November and December 1973, Jet Propulsion Laboratory, Pasadena, California, pp. 31–35, February 15, 1974.
http://ipnpr.jpl.nasa.gov/progress_report2/XIX/XIXF.PDF
- [20] X X Newhall, R. A. Preston, and P. B. Esposito, "Relating the JPL VLBI Reference Frame and the Planetary Ephemerides," *Astrometric Techniques, Proceedings of the 109th IAU Symposium*, H. K. Eichhorn and R. J. Leacock, eds., pp. 789–794, Gainesville, Florida, January 9–12, 1984, Dordrecht, The Netherlands: D. Reidel, 1986.
- [21] J. S. Border, "Innovations in Delta Differential One-way Range: from Viking to Mars Science Laboratory," *Proceedings of the 21st International Symposium on Space Flight Dynamics*, Toulouse, France, September 28–October 2, 2009.
- [22] J. K. Miller and K. H. Rourke, "The Application of Differential VLBI to Planetary Approach Orbit Determination," *The Deep Space Network Progress Report*, vol. 42-40, May and June 1977, Jet Propulsion Laboratory, Pasadena, California, pp. 84–90, August 15, 1977.
http://ipnpr.jpl.nasa.gov/progress_report2/42-40/40J.PDF
- [23] W. G. Melbourne and D. W. Curkendall, "Radiometric Direction Finding: A New Approach to Deep Space Navigation," presented at the AAS/AIAA Astrodynamics Specialist Conference, Jackson Hole, Wyoming, September 7–9, 1977.
- [24] C. Ma, Chairman, *The Second Realization of the International Celestial Reference Frame by Very Long Baseline Interferometry*, IERS Technical Note No. 35, Verlag des Bundesamts für Kartographie und Geodäsie, Frankfurt am Main 2009.
- [25] T. D. Moyer, *Formulation for Observed and Computed Values of Deep Space Network Data Types for Navigation*, JPL Deep Space Communications and Navigation Series, Hoboken, New Jersey: Wiley, 2003.

- [26] T.-H. You, "Mars Reconnaissance Orbiter Interplanetary Cruise Navigation," *Proceedings of the 20th International Symposium on Space Flight Dynamics*, Annapolis, Maryland, September 24–28, 2007.
- [27] B. G. Clark, "The NRAO Tape-Recorder Interferometer System," *Proceedings of the IEEE*, vol. 61, no. 9, pp. 1242–1248, September 1973.
- [28] J. S. Border, F. F. Donovan, S. G. Finley, C. E. Hildebrand, B. Moultrie, and L. J. Skjerve, "Determining Spacecraft Angular Position with Delta VLBI: The Voyager Demonstration," AIAA-82-1471, presented at the AIAA/AAS Astrodynamics Conference, San Diego, California, August 9–11, 1982.
- [29] D. S. Brown, C. E. Hildebrand, and L. J. Skjerve, "Wideband Δ VLBI for Deep Space Navigation," *Proceedings of the IEEE Position Location and Navigation Symposium*, pp. 389–396, Atlantic City, New Jersey, December 1980.
- [30] T. H. Taylor, J. K. Campbell, R. A. Jacobson, B. Moultrie, R. A. Nichols Jr., and J. E. Riedel, "Performance of Differenced Range Data Types in Voyager Navigation," *The Telecommunications and Data Acquisition Progress Report*, vol. 42-71, July and September 1982, Jet Propulsion Laboratory, Pasadena, California, pp. 40–52, November 15, 1982.
http://ipnpr.jpl.nasa.gov/progress_report/42-71/71F.PDF
- [31] F. F. Donovan and X. X. Newhall, "Delta VLBI Observations of Mars Viking Lander I," *Bulletin of the American Astronomical Society*, vol. 13, p. 555, March 1981.
- [32] J. H. Wilcher, "Block I, Phase I Very Long Baseline Interferometry Implementation," *The Telecommunications and Data Acquisition Progress Report*, vol. 42-58, May and June 1980, Jet Propulsion Laboratory, Pasadena, California, pp. 24–27, August 15, 1980.
http://ipnpr.jpl.nasa.gov/progress_report/42-58/58F.PDF
- [33] K. M. Liewer, "DSN Very Long Baseline Interferometry System Mark IV-88," *The Telecommunications and Data Acquisition Progress Report*, vol. 42-93, January–March 1988, Jet Propulsion Laboratory, Pasadena, California, pp. 239–246, May 15, 1988.
http://ipnpr.jpl.nasa.gov/progress_report/42-93/93U.PDF
- [34] E. J. Graat, M. S. Ryne, J. S. Border, and D. B. Engelhardt, "Contribution of Doppler and Interferometric Tracking During the Magellan Approach to Venus," AAS-91-394, *Advances in the Astronautical Sciences*, vol. 76, part II, B. Kaufman, et al., eds., *Proceedings of the AAS/AIAA Astrodynamics Conference*, pp. 919–939, Durango, Colorado, August 19–22, 1991: Univeldt, 1992.
- [35] R. A. Jacobson, R. J. Haw, T. P. McElrath, and P. G. Antreasian, "A Comprehensive Orbit Reconstruction for the Galileo Prime Mission in the J2000 System," AAS-99-330, *Advances in the Astronautical Sciences*, vol. 103, part I, K. C. Howell, et al., eds., *Proceedings of the AAS/AIAA Astrodynamics Conference*, pp. 465–486, Girdwood, Alaska, August 16–19, 1999: Univeldt, 2000.

- [36] L. A. Cangahuala, E. J. Graat, D. C. Roth, S. W. Demcak, P. B. Esposito and R. A. Mase, "Mars Observer Interplanetary Cruise Orbit Determination," AAS-94-133, *Advances in the Astronautical Sciences*, vol. 87, part II, J. E. Cochran Jr., et al., eds., *Proceedings of the AAS/AIAA Spaceflight Mechanics Meeting*, pp. 1049–1068, Cocoa Beach, Florida, February 14–16, 1994: Univeldt, 1994.
- [37] A. G. Stephenson, Chairman, "Mars Climate Orbiter Mishap Investigation Board Phase I Report," National Aeronautics and Space Administration, Washington, D.C., November 10, 1999.
ftp://ftp.hq.nasa.gov/pub/pao/reports/1999/MCO_report.pdf
- [38] P. G. Antreasian, D. T. Baird, J. S. Border, P. D. Burkhart, E. J. Graat, M. K. Jah, R. A. Mase, T. P. McElrath, and B. M. Portock, "2001 Mars Odyssey Orbit Determination During Interplanetary Cruise," *Journal of Spacecraft and Rockets*, vol. 42, no. 3, pp. 394–405, May–June 2005.
- [39] M. P. Golombek, J. A. Grant, T. J. Parker, D. M. Kass, J. A. Crisp, S. W. Squyres, A. F. C. Haldemann, M. Adler, W. J. Lee, N. T. Bridges, R. E. Arvidson, M. H. Carr, R. L. Kirk, P. C. Knocke, R. B. Roncoli, C. M. Weitz, J. T. Schofield, R. W. Zurek, P. R. Christensen, R. L. Fergason, F. S. Anderson, and J. W. Rice, Jr., "Selection of the Mars Exploration Rover Landing Sites," *Journal of Geophysical Research: Planets*, vol. 108, no. E12, 8072, December 2003.
- [40] T. P. McElrath, W. M. Watkins, B. M. Portock, E. J. Graat, D. T. Baird, G. G. Wawrzyniak, A. A. Attiyah, J. R. Guinn, P. G. Antreasian, R. C. Baalke, and W. L. Taber, "Mars Exploration Rovers Orbit Determination Filter Strategy," AIAA-2004-4982, presented at the AIAA/AAS Astrodynamics Conference, Providence, Rhode Island, August 15–20, 2004.
- [41] J. S. Border, "A Global Approach to Delta Differential One-way Range," *Proceedings of 25th International Symposium on Space Technology and Science and 19th International Symposium on Space Flight Dynamics*, paper 2006-d-49, Kanazawa, Japan, June 4–11, 2006.
- [42] M. S. Ryne, E. Graat, R. Haw, G. Kruizinga, E. Lau, T. Martin-Mur, T. McElrath, S. Nandi, and B. Portock, "Orbit Determination for the 2007 Mars Phoenix Lander," AIAA-2008-7215, presented at the AIAA/AAS Astrodynamics Conference, Honolulu, Hawaii, August 18–21, 2008.
- [43] R. Madde, T. Morley, M. Lanucara, R. Abello, M. Mercolino, J. De Vicente, and G. M. A. Sessler, "A Common Receiver Architecture for ESA Radio Science and Delta-DOR Support," *Proceedings of the IEEE*, vol. 95, no. 11, pp. 2215–2223, November 2007.
- [44] H. Takeuchi, S. Horiuchi, C. Phillips, P. Edwards, J. McCallum, J. Dickey, S. Ellingsen, T. Yamaguchi, R. Ichikawa, K. Takefuji, S. Kurihara, B. Ichikawa, M. Yoshikawa, A. Tomiki, and H. Sawada, "Delta-DOR Observations for the IKAROS Spacecraft," paper 2011-o-4-14v, 28th International Symposium on Space Technology and Science, Okinawa, Japan, June 2011. <http://archive.ists.or.jp/>
- [45] D. W. Curkendall, "Radio Metric Technology for Deep Space Navigation: A Development Overview," AIAA-78-1395, presented at the AIAA/AAS Astrodynamics Conference, Palo Alto, California, August 7–9, 1978.

- [46] B. K. Trinkle and S. M. Lichten, "Differential Very Long Baseline Interferometry for 50 Nanoradian Deep Space Navigation: Results from the Quasar Pair Experiments," AAS-85-311, *Advances in the Astronautical Sciences*, vol. 58, part II, B. Kaufman et al., eds, *Proceedings of the AAS/AIAA Astrodynamics Conference*, pp. 1257–1267, Vail, Colorado, August 12–15, 1985: Univeldt, 1986.
- [47] T. T. Pham, S. Shambayati, D. E. Hardi, and S. G. Finley, "Tracking the Galileo Spacecraft With the DSCC Galileo Telemetry Prototype," *The Telecommunications and Data Acquisition Progress Report*, vol. 42-119, July–September 1994, Jet Propulsion Laboratory, Pasadena, California, pp. 221–235, November 15, 1994.
http://ipnpr.jpl.nasa.gov/progress_report/42-119/119R.pdf
- [48] A. Jongeling, E. Sigman, R. Navarro, C. Goodhart, S. Rogstad, K. Chandra, S. Finley, J. Trinh, M. Soriano, L. White, R. Proctor, and B. Rayhrer, *Digital Front End for Wide-Band VLBI Science Receiver*, NASA Tech Brief NPO-41191, September 2006.
<http://ntrs.nasa.gov/search.jsp?R=20110013048>
- [49] P. W. Kinman, "Delta-Differential One-way Ranging," in *DSN Telecommunications Link Design Handbook*, DSN No. 810-005, Module 210, Jet Propulsion Laboratory, Pasadena, California, 2004.
<http://deepspace.jpl.nasa.gov/dsndocs/810-005/210/210.pdf>
- [50] "First Extension of the ICRF, ICRF-Ext. 1," *1998 IERS Annual Report*, Chapter VI (D. Gambis, ed.), Observatoire de Paris, pp. 87–114, 1999.
- [51] J. S. Border, G. E. Lanyi, and D. K. Shin, "Radiometric Tracking for Deep Space Navigation," AAS-08-052, *Advances in the Astronautical Sciences*, vol. 131, M. E. Drews and R. D. Culp, eds., *Proceedings of the AAS Guidance and Control Conference*, Breckenridge, Colorado, February 1–6, 2008: Univeldt, 2008.
- [52] Y. E. Bar-Sever, C. S. Jacobs, S. Keihm, G. E. Lanyi, C. J. Naudet, H. W. Rosenberger, T. F. Runge, A. B. Tanner, and Y. Vigue-Rodi, "Atmospheric Media Calibration for the Deep Space Network," *Proceedings of the IEEE*, vol. 95, no. 11, pp. 2180–2192, November 2007.
- [53] A. J. Mannucci, B. D. Wilson, D. N. Yuan, C. H. Ho, U. J. Lindqwister, and T. F. Runge, "A Global Mapping Technique for GPS-Derived Ionospheric Total Electron Content Measurements," *Radio Science*, vol. 33, no. 3, pp. 565–582, May–June 1998.
- [54] R. S. Gross, "Earth Rotation Variations — Long Period," in *Physical Geodesy*, T. A. Herring, ed., *Treatise on Geophysics*, vol. 11, Amsterdam, The Netherlands: Elsevier, 2007.
- [55] C. S. Jacobs, "X-Band Radio Source Catalog," in *DSN Telecommunications Link Design Handbook*, DSN No. 810-005, Module 107B, Jet Propulsion Laboratory, Pasadena, California, 2013.
<http://deepspace.jpl.nasa.gov/dsndocs/810-005/107/107B.pdf>
- [56] W. Majid and D. Bagri, "Availability of Calibration Sources for Measuring Spacecraft Angular Position with Sub-Nanoradian Accuracy," *The Interplanetary Network Progress Report*, vol. 42-165, Jet Propulsion Laboratory, Pasadena, California, pp. 1–8, May 15, 2006. http://ipnpr.jpl.nasa.gov/progress_report/42-165/165D.pdf

- [57] S. T. Lowe, "A Measurement of X-Band Front-End Phase Dispersion for Delta-Differenced One-Way Range (DDOR) Experiments," *The Interplanetary Network Progress Report*, vol. 42-184, Jet Propulsion Laboratory, Pasadena, California, pp. 1–15, February 15, 2011.
http://ipnpr.jpl.nasa.gov/progress_report/42-184/184B.pdf
- [58] W. A. Majid and D. S. Bagri, "Precision Relative Astrometry with the Deep Space Network," *The Interplanetary Network Progress Report*, vol. 42-172, Jet Propulsion Laboratory, Pasadena, California, pp. 1–17, February 15, 2008.
http://ipnpr.jpl.nasa.gov/progress_report/42-172/172A.pdf
- [59] G. Lanyi, "Quadruply Differenced One-Way Ranging: QDOR," *The Interplanetary Network Progress Report*, vol. 42-186, Jet Propulsion Laboratory, Pasadena, California, pp. 1–15, August 15, 2011.
http://ipnpr.jpl.nasa.gov/progress_report/42-186/186A.pdf
- [60] T. J. Martin-Mur and D. E. Highsmith, "Mars Approach Navigation Using the VLBA," *Proceedings of the 21st International Symposium on Space Flight Dynamics*, Toulouse, France, September 28–October 2, 2009.
- [61] G. E. Lanyi, D. A. Boboltz, P. Charlot, A. L. Fey, E. B. Fomalont, B. J. Geldzahler, D. Gordon, C. S. Jacobs, C. Ma, C. J. Naudet, J. D. Romney, O. J. Sovers, and L. D. Zhang, "The Celestial Reference Frame at 24 and 43 GHz. I. Astrometry," *The Astronomical Journal*, vol. 139, no. 5, pp. 1695–1712, May 2010.
- [62] W. M. Folkner, P. Charlot, M. H. Finger, J. G. Williams, O. J. Sovers, X X Newhall, and E. M. Standish Jr., "Determination of the Extragalactic-Planetary Frame Tie from Joint Analysis of Radio Interferometric and Lunar Laser Ranging Measurements," *Astronomy and Astrophysics*, vol. 287, no. 1, pp. 279–289, July 1994.